


RESEARCH

Open Access



The amyloid plaque proteome in early onset Alzheimer's disease and Down syndrome

Eleanor Drummond^{1,2*}, Tomas Kavanagh¹, Geoffrey Pires², Mitchell Marta-Ariza², Evgeny Kanshin³, Shruti Nayak⁴, Arline Faustin², Valentin Berdah², Beatrix Ueberheide^{2,3,5} and Thomas Wisniewski^{2,6*} 

Abstract

Amyloid plaques contain many proteins in addition to beta amyloid (A β). Previous studies examining plaque-associated proteins have shown these additional proteins are important; they provide insight into the factors that drive amyloid plaque development and are potential biomarkers or therapeutic targets for Alzheimer's disease (AD). The aim of this study was to comprehensively identify proteins that are enriched in amyloid plaques using unbiased proteomics in two subtypes of early onset AD: sporadic early onset AD (EOAD) and Down Syndrome (DS) with AD. We focused our study on early onset AD as the drivers of the more aggressive pathology development in these cases is unknown and it is unclear whether amyloid-plaque enriched proteins differ between subtypes of early onset AD. Amyloid plaques and neighbouring non-plaque tissue were microdissected from human brain sections using laser capture microdissection and label-free LC-MS was used to quantify the proteins present. 48 proteins were consistently enriched in amyloid plaques in EOAD and DS. Many of these proteins were more significantly enriched in amyloid plaques than A β . The most enriched proteins in amyloid plaques in both EOAD and DS were: COL25A1, SMOC1, MDK, NTN1, OLFML3 and HTRA1. Endosomal/lysosomal proteins were particularly highly enriched in amyloid plaques. Fluorescent immunohistochemistry was used to validate the enrichment of four proteins in amyloid plaques (moesin, ezrin, ARL8B and SMOC1) and to compare the amount of total A β , A β 40, A β 42, phosphorylated A β , pyroglutamate A β species and oligomeric species in EOAD and DS. These studies showed that phosphorylated A β , pyroglutamate A β species and SMOC1 were significantly higher in DS plaques, while oligomers were significantly higher in EOAD. Overall, we observed that amyloid plaques in EOAD and DS largely contained the same proteins, however the amount of enrichment of some proteins was different in EOAD and DS. Our study highlights the significant enrichment of many proteins in amyloid plaques, many of which may be potential therapeutic targets and/or biomarkers for AD.

Keywords: Alzheimer's disease, Amyloid plaques, Amyloid beta, Proteomics, Early onset, Down syndrome, Mass spectrometry

Introduction

Amyloid plaques are a neuropathological hallmark of Alzheimer's disease and primarily consist of the protein beta amyloid (A β). However, it is often overlooked that amyloid plaques also contain hundreds of proteins in addition to A β . These include proteins that directly interact with A β (e.g. apolipoprotein E [1]), proteins present in microglia and astrocytes that surround and infiltrate plaques, and proteins present in dystrophic neurites (e.g. phosphorylated tau [2], neurofilament proteins [3],

*Correspondence: Eleanor.drummond@sydney.edu.au; Thomas.Wisniewski@nyulangone.org

¹ Brain and Mind Centre and School of Medical Sciences, Faculty of Medicine and Health, University of Sydney, 94 Mallett Street, Camperdown, NSW, Australia

² Centre for Cognitive Neurology, Department of Neurology, New York University Grossman School of Medicine, Science Building, Rm 1017, 435 East 30th Street, New York, NY 10016, USA

Full list of author information is available at the end of the article



secernin-1 [4]). Previous studies have shown that many of these plaque proteins have mechanistic roles in AD. For example, proteins that directly interact with A β influence A β aggregation and therefore mediate amyloid plaque formation [5–7]. The proteins present in plaque-associated glia influence glial function and can mediate pathological glial function [8, 9]. Proteins present in dystrophic neurites provide insight into the factors involved in the formation of dystrophic neurites and neuritic plaques, which correlate better with cognitive impairment than diffuse plaques [10]. Therefore, comprehensively profiling the proteins that are enriched in amyloid plaques would increase our understanding about AD pathogenesis, and possibly identify new biomarkers and/or new therapeutic targets for AD.

Previous studies have typically used immunohistochemistry to identify amyloid plaque proteins. Mass spectrometry-based proteomics is an alternative approach that allows efficient quantification of thousands of amyloid plaque proteins simultaneously. Proteomics also offers additional advantages of allowing discovery of novel plaque proteins due to its unbiased nature and bypassing complications due to antibody sensitivity and specificity issues. Given these significant advantages, we recently developed a localized proteomics approach to analyze the proteome of neuropathological lesions in AD such as plaques and neurofibrillary tangles [11–13].

The significant heterogeneity in the clinical and neuropathological phenotype of AD suggests that multiple subtypes of AD exist. Previous studies have used various approaches to define AD subtypes [14–17]. Some studies have defined AD subtypes by age of onset (e.g. early onset vs late onset), genetics (e.g. apoE2 vs apoE3 vs apoE4 or familial AD vs sporadic AD), by neuropathology phenotype (e.g. limbic predominant vs hippocampal sparing vs typical), by rate of progression (e.g. rapidly progressive AD vs typical AD), or more recently using unbiased ‘omics approaches. We recently showed that plaques in rapidly progressive AD had a significantly different proteome than plaques in typical sporadic AD, suggesting that the amyloid plaque proteome is not consistent in all AD subtypes and that these plaque protein differences may contribute to the development of different subtypes of AD [11]. It is currently unclear whether amyloid plaques in other AD subtypes also have significantly different protein composition, or whether these plaque protein differences were unique to rapidly progressive AD.

The aim of this study was to compare the amyloid plaque proteome in two subtypes of early onset AD: sporadic early onset AD (EOAD) and Down Syndrome (DS) with AD. Between 5 and 10% of AD cases are considered early onset [18]. Of these, only approximately 10% are caused by *APP*, *PSEN1* and *PSEN2* mutations. The

cause of the remaining ~90% of EOAD cases is unknown and these cases are therefore characterized as sporadic EOAD. It is currently unclear if the same molecular mechanisms drive sporadic EOAD cases and late-onset AD [18]. DS with AD is another prevalent subtype of early onset AD. Adults with DS have a very high risk of developing AD, which is thought to be driven by the triplication and consequent overexpression of APP in DS [19]. People with DS develop AD associated neuropathology very early in life. Accumulation of soluble A β has been observed in fetuses with DS [20]. Intran neuronal A β is present in children as young as 1 year old [21], which is followed by the development of diffuse plaques by the age of approximately 12 years [22, 23]. Mature plaques are commonly present in the 30’s and advanced AD neuropathology is present by the 40’s [24]. The progressive accumulation of amyloid and tau pathology in DS largely follows a similar pattern to that observed in AD [25], albeit with more plaques in the striatum and thalamus [26] and a higher plaque density overall in DS in comparison to AD [27]. Multiple studies have shown that plaques in DS contain similar post-translationally modified A β species as observed in AD, including A β phosphorylated at serine 8 and pyroglutamate modified A β [23, 28–31], however it is still unknown if plaques in DS have a different protein composition to that in AD.

Here, we show that amyloid plaques in DS and EOAD are enriched in many proteins besides A β including a common core group of 48 proteins that are enriched in plaques in both AD subtypes. While similar proteins were enriched in both DS and EOAD, some proteins were enriched to a greater extent in plaques in a particular subtype of AD, providing new evidence that some distinctions in plaque protein composition are present.

Methods

Ethics statement

All procedures were performed under protocols approved by the Institutional Review Board at New York University Alzheimer Disease Center, NY, USA. In all cases, written informed consent for research was obtained from the patient or legal guardian, and the material used had appropriate ethical approval for use in this project. All patients’ data and samples were coded and handled according to NIH guidelines to protect patients’ identities.

Human tissue samples

N=5 cases of early onset sporadic Alzheimer’s disease (EOAD) and n=5 cases of DS with Alzheimer’s disease were included for proteomic experiments. Inclusion criteria for EOAD included age < 65 years, ABC neuropathological score of A3, B3, C3 [32], no

mutation in *APP*, *PSEN1* or *PSEN2*, tissue formalin fixation time <6 months. Inclusion criteria for DS cases was ABC neuropathological score of A3, B3, C3, formalin fixation time <6 months. Formalin fixed paraffin embedded tissue blocks containing the hippocampus and surrounding entorhinal/temporal cortex that were collected and processed as part of routine autopsy procedures were used in this study. This region was selected because it contains a high amount of amyloid pathology in EOAD and in DS with AD. N=3 cases of EOAD, DS, late onset sporadic AD (LOAD) and cognitively normal, age matched controls were included in immunohistochemistry validation studies. Case specific information for the human tissue samples used in this study is included in Table 1.

APOE genotyping

APOE genotyping was performed on all the cases using either formalin-fixed paraffin embedded (FFPE) or frozen tissue (FT) for the cases where it was available (see Table 1). FT is the preferred tissue for genotyping as the results are more reliable using this source, which is less likely to be affected by DNA contamination; however, FT was available only from five cases. For FFPE tissues, DNA was isolated from six 8 µm brain sections per sample, using the automated system QIASymphony SP (Qiagen) and the protocol indicated by the manufacturer. Two endpoint PCRs were performed before sequencing. The

first endpoint PCR was conducted in a total volume of 25 µl containing 0.2 µM of each custom primer (Forward primer 5' AGGCCTACAAATCGGAACTGG 3'; reverse primer 5' CCTGTTCCACCAGGGGC 3'; Sigma), 0.5 mM each dNTP (Thermo Scientific), 2 U GoTaq G2 Hot Start polymerase (Promega), 25 mM MgCl₂ solution (Promega) and 4.2 µl Betaine (Sigma). Cycling conditions were at 98 °C for 4 min and 40 cycles at 98 °C/10 s, 63 °C/1 min and 72 °C/1 min 10 s, followed by 72 °C 10 min. All the amplified fragments were resolved on 2% agarose gels, stained with GelRed 10,000X (Biotium) and visualized under UV exposure. DNA was purified from the agarose gel using the Illustra™ GFX™ PCR DNA and Gel Band Purification Kit (Cytiva) as indicated by the manufacturer, and DNA concentration was quantified using nanodrop One (Thermo Scientific). The second endpoint PCR was performed using the purified DNA with the conditions described previously, except for the concentration of the primers, which was reduced to 0.15 µM. Unpurified PCR products were submitted to Genewiz for Sanger sequencing, and the sequences were analyzed using SnapGene 5.3.1 software (Additional File 2). For genotyping using frozen tissue, 25 mg were dissected from the brain section and transferred to a 1.5 ml tube. DNA was isolated using the DNeasy Blood & Tissue kit (Qiagen) following the manufacturer's instructions. A single endpoint PCR was performed in a total volume of 25 µl containing 0.2 µM of each custom primer (Forward

Table 1 Human tissue samples used in this study

Patient ID	Sex	Age at death	APOE genotype on FFPE or FT	ABC score	Fixation duration in weeks	Inclusion in proteomics study	Inclusion in IHC studies	Number of plaques micro-dissected	Number of non-plaques micro-dissected
EOAD #1	F	55	ε3/ε3; FFPE	A3, B3, C3	2	Yes	Yes	641	643
EOAD #2	M	62	ε3/ε3; FT	A3, B3, C3	3	Yes	Yes	622	622
EOAD #3	M	63	ε3/ε3; FFPE	A3, B3, C3	2	Yes	Yes	644	648
EOAD #4	M	63	ε4/ε4; FT	A3, B3, C3	3	Yes	Yes	627	627
EOAD #5	F	60	ε3/ε4; FT	A3, B3, C3	3	Yes	Yes	680	680
EOAD #6	M	70	ε3/ε3; FFPE	A3, B3, C3	2		Yes	n/a	n/a
EOAD #7	F	70	ε3/ε3; FFPE	A3, B3, C3	2		Yes	n/a	n/a
DS #1	F	58	ε3/ε3; FFPE	A3, B3, C3	2	Yes	Yes	607	607
DS #2	M	55	ε3/ε4; FFPE	A3, B3, C3	2	Yes	Yes	641	641
DS #3	M	54	ε3/ε3; FFPE	A3, B3, C3	2	Yes	Yes	603	603
DS #4	F	59	ε3/ε3; FFPE	A3, B3, C3	2	Yes	Yes	633	633
DS #5	F	37	ε3/ε3; FFPE	A3, B3, C3	2	Yes	Yes	626	624
LOAD #1	M	76	ε3/ε4; FT	A3, B3, C3	3		Yes	n/a	n/a
LOAD #2	M	77	ε3/ε3; FFPE	A3, B3, C3	3		Yes	n/a	n/a
LOAD #3	F	88	ε3/ε4; FT	A3, B3, C3	2		Yes	n/a	n/a
Control #1	M	59	ε3/ε3; FFPE	A1, B1, C0	3		Yes	n/a	n/a
Control #2	F	77	ε3/ε3; FFPE	A1, B1, C1	2		Yes	n/a	n/a
Control #3	F	71	ε3/ε3; FFPE	A1, B1, C0	2		Yes	n/a	n/a

primer 5' AGCCCTTCTCCCCGCCTCCCACTGT 3'; reverse primer 5' CTCCGCCACCTGCTCCTTACCTCG 3'; Sigma), 10 μ l of DreamTaq Green PCR Master Mix (2X) and 4.2 μ l Betaine (Sigma). Cycling conditions were at 98 °C for 4 min and 35 cycles at 98 °C/10 s, 63 °C/45 s and 72 °C/1 min 10 s, followed by 72 °C 10 min. Unpurified PCR products were submitted to Genewiz for Sanger sequencing, and the sequences were analyzed using SnapGene 5.3.1 software.

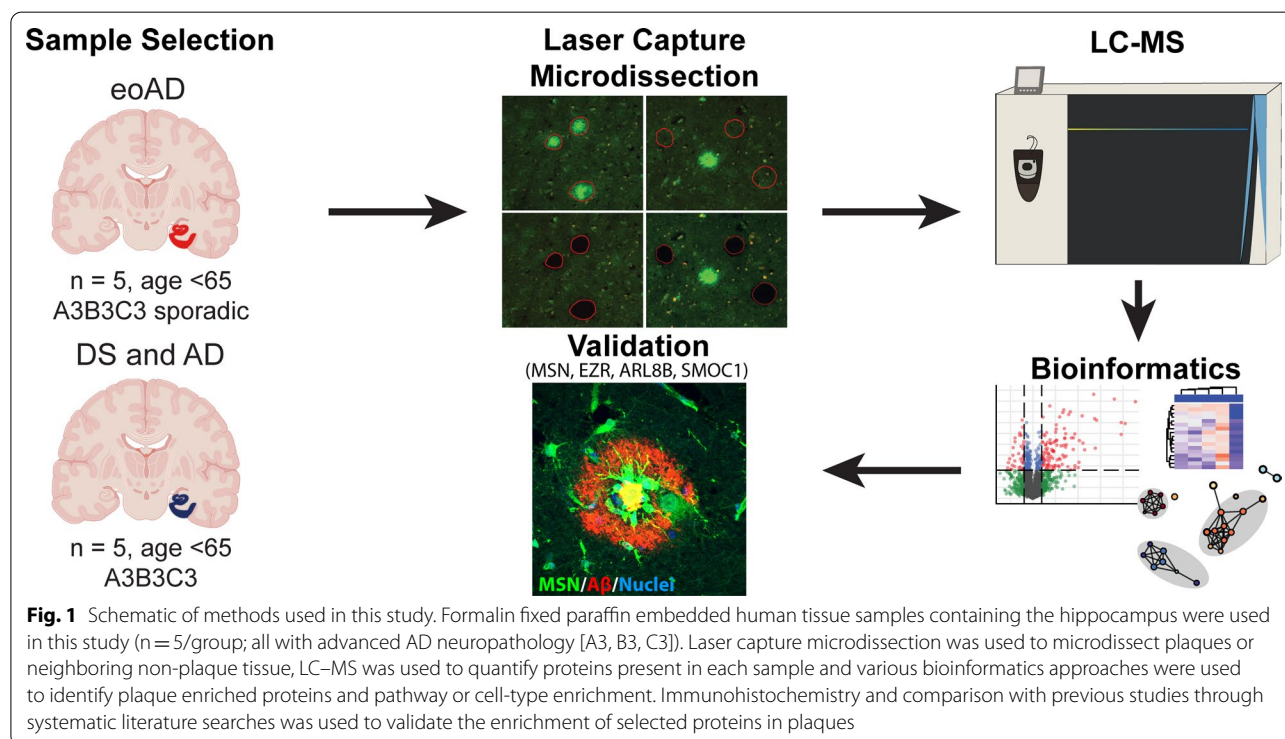
Immunohistochemistry for A β species

8 μ m formalin-fixed paraffin embedded tissue sections containing the hippocampus and surrounding cortex underwent fluorescent immunohistochemistry for six different A β species: total A β (combination of 4G8 [BioLegend; #800701] and 6E10 [BioLegend; #803001]), A β 40 (in-house developed monoclonal rabbit antibody [33]), A β 42 (in-house developed monoclonal rabbit antibody [33]), A β phosphorylated at serine position 8 (pA β ; in-house developed monoclonal mouse antibody), pyroglutamate modified A β (pyro-A β ; [34]), and the conformational oligomeric antibody TWF9 [35] that recognizes beta-sheet containing oligomeric species including A β . Sections were deparaffinized and rehydrated through a series of xylene and ethanol washes. Antigen retrieval was performed by treatment with either 88% formic acid for 7 min followed by boiling in citrate buffer (10 mM sodium citrate, 0.05% Tween-20; pH6) for total A β , A β 42,

A β 40, pyro-A β or with citrate buffer alone for pA β and TWF9. Sections were blocked with 10% normal goat serum, incubated overnight primary antibodies diluted in 4% normal goat serum. Sections were incubated for 2 h at room temperature with appropriate fluorescent secondary antibodies (diluted 1:500, from Jackson ImmunoResearch). Sections were counter stained with Hoechst 33342 (Sigma) and coverslipped (Prolong Diamond, Thermo Fisher Scientific). Whole slide images were generated using a NanoZoomer HT2 (Hamamatsu) slide scanner. Eight 4 \times magnification images were collected for quantification from the whole slide scans: four containing the cortex, one each of CA1, CA2, CA3 and CA4, which together generated an average percentage staining load per case. Quantification of the percentage staining load was performed using ImageJ by quantifying the number of pixels above a defined staining threshold for each marker. The percentage staining load of total A β , A β 42, A β 40, phosphorylated A β and pyroglutamate A β abundance was restricted to staining in amyloid plaques only, while percentage staining load of oligomers refers to levels throughout the cortical grey matter. Significant differences were determined by one-way ANOVA followed by Tukey's multiple comparisons test.

Laser capture microdissection for localized proteomics

Proteomic studies were carried out using the method outlined in Fig. 1. 8 μ m sections of formalin-fixed paraffin



embedded tissue were collected onto laser capture microdissection (LCM)-compatible slides and amyloid plaques were visualized using fluorescent immunohistochemistry using a combination of the pan-A β antibodies 4G8 (1:4000; BioLegend; #800701) and 6E10 (1:4000; BioLegend; #803001). LCM was performed using a LMD 6500 microscope (Leica) using the method detailed in [11, 36]. 2 mm² total area of fluorescently-labelled plaques was microdissected using LCM for each case. 2 mm² total area of neighboring non-plaque tissue was also collected for each case. Non-plaque tissue was only selected from the same microscopic field of views that contained microdissected plaques, while remaining sufficiently distant from plaques to ensure that plaque-associated tissue was not collected (Fig. 1). The same number of microdissected regions were collected for plaques and non-plaques for each sample to control for proteomic variation based on the tissue loss associated with microdissection. The inclusion criteria for plaques in this study was any plaque visualized by IHC. There was no restriction based on plaque morphology. Plaques were microdissected from any region present on the hippocampal section, which included hippocampus, entorhinal cortex and temporal cortex. Plaques or non-plaque regions were collected into double distilled water and stored at -80 °C until sample processing for LC-MS.

Localized proteomics of amyloid plaques

Samples were processed for LC-MS/MS using the formic acid sample preparation method we have previously used to analyze the proteome of amyloid plaques [11, 13, 37]. Tissue underwent secondary deparaffinization using a heating protocol (95 °C for one hour and 65 °C for 2 h and were incubated in 70% LC-MS grade formic acid overnight at room temperature. Samples were sonicated (3 × 3 min), dried using a SpeedVac concentrator, resuspended in 100 mM ammonium bicarbonate and then reduced with Dithiothreitol (20 mM) and alkylated with iodoacetamide (50 mM). Samples were digested with sequencing grade modified trypsin (200 ng; Promega) by gentle agitation overnight at room temperature. Samples were acidified with 0.2% TFA and peptides were desalted using Poros beads. Peptides were eluted off the beads by addition of 40% acetonitrile in 0.5% acetic acid followed by the addition of 80% acetonitrile in 0.5% acetic acid. The organic solvent was removed using a SpeedVac concentrator and the samples were reconstituted in 0.5% acetic acid.

One third of each sample was loaded onto the column using the auto sampler of an EASY-nLC 1200 HPLC (ThermoFisher). The peptides were gradient eluted directly into an Orbitrap Fusion Lumos mass spectrometer using a 145-min gradient. The Orbitrap Fusion

Lumos mass spectrometer acquired high resolution full MS spectra with a resolution of 240,000 (at m/z 200), AGC target of 1e6, with a maximum ion time of 50 ms, and scan range of 400–1500 m/z. Following each full MS data-dependent low resolution HCD MS/MS spectra were acquired. All MS/MS spectra were collected using the following instrument parameters: rapid ion trap scan rate, ACG target of 2e4, maximum ion time of 150 ms, one microscan, 0.7 m/z isolation window, fixed first mass of 150 m/z and NCE of 32.

LC-MS data analysis

Protein quantitation was performed using MaxQuant software suite v. 1.6.3.4 [38]. Raw data generated by match between runs. The MS/MS spectra were searched against the SwissProt subset of the Uniprot *H. Sapiens* proteome database (26,186 entries) using the Andromeda search engine [39]. A list of 248 common laboratory contaminants included in MaxQuant, as well as reversed versions of all sequences were also added to the database. The enzyme specificity was set to trypsin with a maximum number of missed cleavages set to 2. Peptide identification was performed with an initial precursor mass deviation up to 7 ppm and a fragment mass deviation of 20 ppm with subsequent nonlinear mass recalibration. Oxidation of methionine and acetylation of protein NTerm were searched as variable modifications and carbamidomethylation of cysteines was searched as a fixed modification. The false discovery rate (FDR) for peptide, protein, and site identification was set to 1% and was calculated using a decoy database approach. The minimum peptide length was set to 7. The option match between runs (1 min time tolerance) was enabled to correlate identification and quantitation results across different runs. Normalization for label-free quantification was performed using MaxLFQ algorithm [38]. Missing values were imputed from normal distribution in Perseus [40] using default parameters. The final protein list was filtered to only include proteins that were present in at least 3 cases in at least one experimental group. An independent quantification for A β was manually curated and included in the search results, consistent with previous studies [41]. To do this, the intensity for A β was determined by integrating the area under the curve for peptide LVFFAEDVGSNK, which corresponds to amino acids 17–28 of A β .

Plaque enriched/depleted proteins were determined as those with a fold change difference between plaques and non-plaques > 1.5 fold and an uncorrected *p* value of *p* < 0.05 (paired *t*-test). Fold change difference was selected as the primary determinant of enrichment/depletion in plaques as this correlated best with immunohistochemistry studies, which is the gold standard

approach for identifying plaque enriched proteins. Uncorrected p -values were included to provide an indication of variance within a group, however plaque-enriched proteins identified by p -values alone did not correlate as well with prior gold-standard immunohistochemistry studies.

Direct comparison of plaque protein levels in DS and EOAD was performed using plaque protein levels that were normalized to the neighboring non-plaque tissue for each individual case. For this, normalized plaque protein levels were calculated as the ratio of protein intensity in plaques:non-plaques for each case. Differences in normalized plaque protein levels between DS and EOAD were identified using an unpaired t -test and proteins were deemed significantly different based on a combination of $p < 0.05$ and fold change difference > 1.5 .

Data analysis and figure generation

General data manipulations and grouping were performed in R v4.0.2 [42] using the tidyverse v1.3.0 collection of packages. Plots were generated in R with the packages ggplot2 v3.3.2, ggpubr v0.4.0, ggrepel v0.8.2, EnhancedVolcano v1.6.0, VennDiagram v1.6.20, ComplexHeatmap v2.4.3, circlize v0.4.10 and edited in Adobe Illustrator v25.2.3. KEGG pathways and Gene Ontology enrichment analysis was performed in R using the packages enrichplot v1.8.1, DOSE v3.14.0, clusterProfiler v3.16.1, GOsemSim v2.14.2 with terms filtered to an FDR < 0.05 . Heatmaps were created with scaled data using the scale function in R. Protein–protein interaction networks and gene ontology cellular compartment annotations were generated in STRING v11.0 [43] and the networks were edited in Cytoscape v3.8.1 and Adobe Illustrator.

Comparison with previous studies

Systematic literature searches were used to identify plaque enriched proteins that have been validated in previous studies. A protein was designated a “known plaque protein” if there was published evidence of enrichment in amyloid plaques in human tissue using immunohistochemistry or mass spectrometry. Additional literature searches were used to determine if a protein was functionally associated with either A β or APP in instances where there was no immunohistochemistry evidence of presence in plaques. Key words used in these pubmed searches were: “Alzheimer’s and gene ID” or “Alzheimer’s and protein name”. Plaque enriched proteins identified by mass spectrometry were determined by comparison with Xiong et al. [44], which is the only previous study to identify plaque enriched proteins in comparison to non-plaque regions in human brain tissue using mass spectrometry. Published data from Xiong et al. was filtered

to identify plaque-enriched proteins that were identified by at least 2 peptides, had a fold-change difference of > 1.5 fold between plaques and non-plaques for AD versus controls or preclinical AD versus controls and did not include the word “keratin” or “immunoglobulin” in the protein name to make their data comparable with ours. Proteins with an abundance in the bottom 10% in sAD plaques or preclinical plaques were excluded. Uniprot ID was used to match proteins between studies.

Change in brain protein expression in AD versus controls was determined using our in-house developed database—NeuroPro—which combines results from 33 previous studies that used proteomics to identify consistent protein differences between AD and control human brain tissue [11, 12, 41, 44–73].

Validation immunohistochemistry

Proteins were selected for validation studies based on the following criteria: enrichment in both EOAD and DS plaques, protein abundance in the top 50% in amyloid plaques, high fold change enrichment in plaques, appropriate commercial antibody available and limited/no previous evidence of presence in plaques by immunohistochemistry. Based on these criteria the following proteins were selected for immunohistochemistry validation studies: MSN, EZR, SMOC1 and ARL8B. 8 μ m formalin-fixed paraffin embedded tissue sections containing the hippocampus and surrounding cortex were used for immunohistochemistry validation studies using the fluorescent immunohistochemistry method described above. Primary antibodies used for these validation studies included: MSN (1:200; Proteintech; #16495-1-AP), EZR (1:100; Thermo Scientific; #QG218841), SMOC1 (1:100; Invitrogen; #PA5-31392), ARL8B (1:200; Invitrogen; #PA5-98885), A β (combination of 4G8 [BioLegend; #800701] and 6E10 [BioLegend; #803001], both 1:4000). The combined formic acid and citrate buffer antigen retrieval method (described above) was used for all validation immunohistochemistry studies. 63 \times images of fluorescent immunohistochemistry were collected using a confocal microscope Zeiss 700 with the ZEN Black 2.3 SP1 acquisition software. ARL8B immunoreactivity in neurons, microglia and astrocytes was tested using the same method as above with the following primary antibodies: GFAP (1:1000; BioLegend; #837201), IBA1 (1:200; Millipore; #MABN92-25UG) and MAP2 (1:300, BD Pharmingen, #556320). A negative control was included in all immunohistochemistry experiments, which consisted of a section of AD hippocampal tissue that underwent the same method with the primary antibody omitted.

The percentage of amyloid plaques co-localized with ARL8B or SMOC1 was quantified using whole slide

fluorescent scans that were collected using the Aperio VERSA digital slide scanner (Leica) with the 10× objective. Images were visualized and analyzed using the software Aperio ImageScope ver. 12.4.3 (Leica). Plaques co-stained with SMOC1 or ARL8B and Aβ or plaques stained only with Aβ in the hippocampal region were manually counted and then the ratio of co-stained plaques versus total plaques was calculated (co-stained plaques/total plaques × 100). The proportion of the plaques was obtained by plotting total number of plaques compared to the plaques co-stained by SMOC1 or ARL8B and Aβ, using the “grouped” layout of GraphPad Prism 8. Significant differences between groups were identified using one-way ANOVA followed by Tukey multiple comparison’s analysis, using GraphPad Prism 8 software.

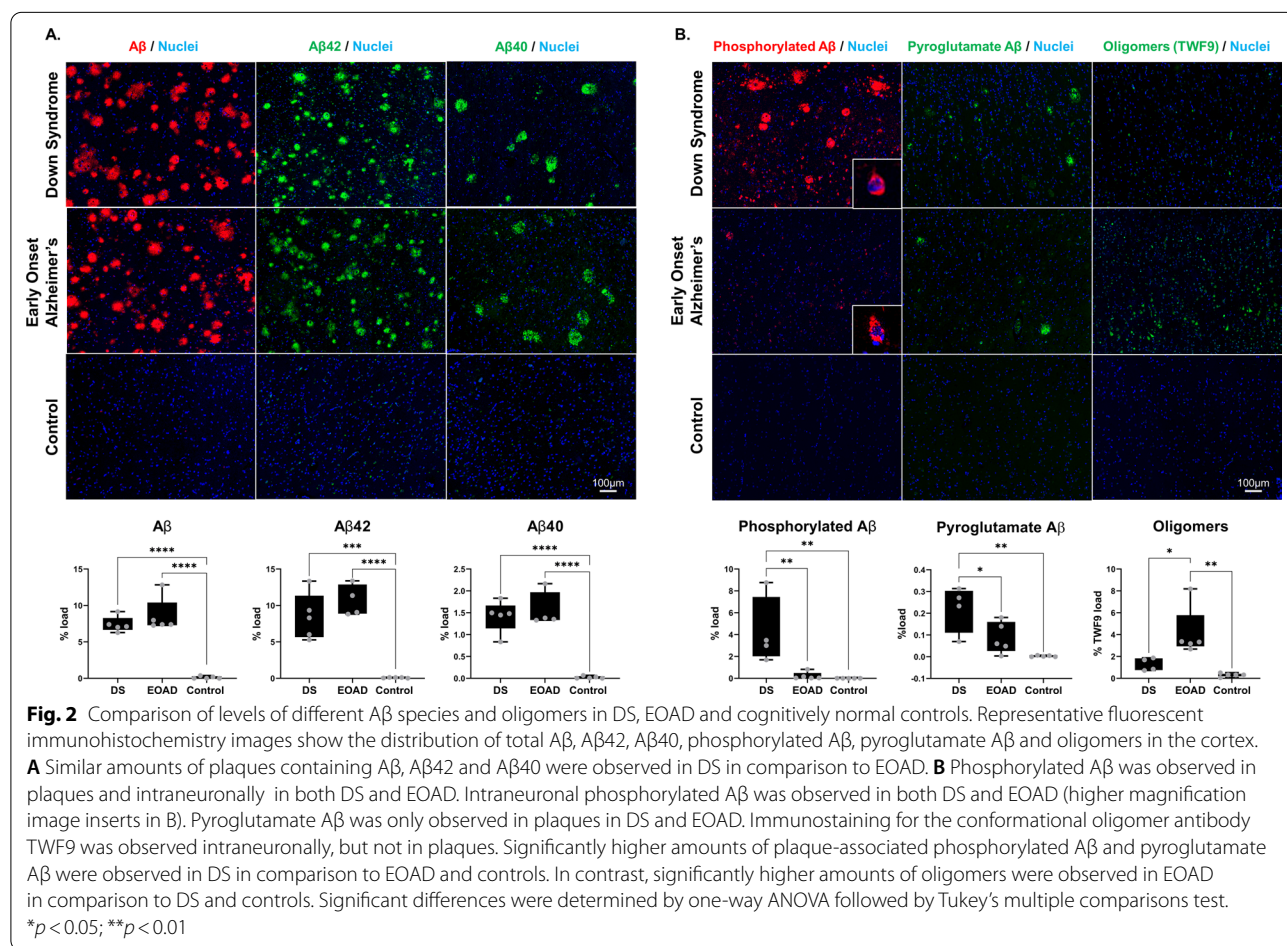
Results

Differences in Aβ species in EOAD and DS

Amyloid plaques in DS and EOAD had similar amounts of total Aβ, Aβ40 and Aβ42 (Fig. 2A). The size of amyloid plaques was similar in DS and EOAD. However, amyloid plaques in DS had significantly higher amounts

of both phosphorylated Aβ and pyroglutamate Aβ than EOAD cases (Fig. 2B). Phosphorylated Aβ immunoreactivity was observed both in plaques and in neurons in DS and EOAD. Two main types of intraneuronal staining were observed: staining consistent with presence in neurofibrillary tangles and neurons containing large puncta of phosphorylated Aβ. Phosphorylated Aβ was also observed in dystrophic neurites. While there were significantly increased levels of phosphorylated Aβ in plaques in DS in comparison to EOAD, similar levels of intraneuronal phosphorylated Aβ were observed in DS and EOAD. Pyroglutamate Aβ was observed in amyloid plaques in both DS and EOAD. Significantly more pyroglutamate Aβ was observed in DS in comparison to EOAD (Fig. 2B).

Oligomers were visualized using the pan-oligomeric antibody TWF9, which is a conformational antibody that recognizes Aβ oligomers in addition to other beta sheet containing oligomers [35]. Consistent with previous studies, TWF9 immunoreactivity was observed in neuronal soma. No immunoreactivity was observed within plaques. DS cases had significantly lower levels



of TWF9 immunoreactivity in comparison to EOAD (Fig. 2B).

Proteomic analysis of EOAD and DS amyloid plaques

Proteomic analysis of plaques and neighboring non-plaque tissue identified 2259 proteins (Additional file 1: Table S1). 85% of proteins (1915 proteins) were identified in both EOAD and DS samples, of which 1355 proteins were identified in all 20 samples, therefore confirming that our proteomic approach is a reliable way to quantify amyloid plaque proteins using microscopic amounts of formalin-fixed paraffin embedded human tissue samples. Proteins present in all 20 samples included major AD-associated proteins such as A β , Tau and ApoE, therefore confirming the presence of these proteins both inside plaques and in surrounding non-plaque tissue.

Proteins enriched in plaques in both EOAD and DS

The main aim of this study was to identify proteins that were enriched in amyloid plaques in EOAD and DS in comparison to surrounding non-plaque tissue. 127 proteins were significantly enriched in amyloid plaques in either EOAD or DS (Additional file 1: Table S1). 48 proteins were consistently enriched in both DS and EOAD plaques (Table 2, Fig. 3). Systematic literature searches revealed that 33/48 proteins have been previously confirmed as amyloid plaque proteins in late-onset AD, therefore validating our mass spectrometry approach and providing new evidence that similar proteins are enriched in amyloid plaques in different subtypes of AD (Table 2). In addition, we identified 15 proteins that were enriched in plaques in both EOAD and DS (Table 2) that were not previously known to be plaque associated proteins. Four of these proteins have been previously associated with either A β or APP. Here, we provide the first evidence that these proteins are enriched in amyloid plaques. The remaining 11 proteins are amyloid plaque proteins that have not been previously associated with A β , APP or amyloid plaques in any subtype of AD (Table 2).

As expected, A β was highly enriched in plaques in comparison to the surrounding non-plaque tissue (12 and sevenfold enriched in EOAD and DS plaques respectively; Fig. 3B). In contrast, while tau was abundant in both plaques and neighboring non-plaque tissue in DS and EOAD, there was no evidence of enrichment of tau in amyloid plaques. Examination of the abundance (overall intensity in plaques) of the 48 proteins enriched in both EOAD and DS showed that the most abundant proteins present were well-known plaque proteins (e.g. APP, ApoE, vimentin, clusterin, complement C3 and complement C4a; Fig. 3C). We also observed a very high correlation in the total concentration of these proteins in plaques between EOAD and DS (Fig. 3C). The most

abundant novel plaque protein in both DS and EOAD was ezrin (EZR), which was one of the proteins selected for immunohistochemistry validation studies (Fig. 3C).

Examination of the proteins that had the highest enrichment in plaques in both DS and EOAD included many proteins less studied in the AD field (Table 2; Additional file 1: Table S3). For example, COL25A1 was the most highly enriched protein in plaques in both EOAD and DS (104 and 113-fold enriched respectively). Other highly enriched plaque proteins in both EOAD and DS included MDK, NTN1, HTRA1, SMOC1 and OLFML3 (Fig. 4A, B). The 48 proteins consistently enriched in plaques in both EOAD and DS also showed a highly significant degree of protein–protein interaction ($p < 1.0 \times 10^{-16}$; Fig. 3D) and were almost exclusively classified as either vesicle (enrichment FDR: 4.32×10^{-9}) or extracellular proteins (enrichment FDR: 3.34×10^{-8}). The enrichment of vesicle proteins was predominantly driven by endosome or lysosome proteins (Fig. 3D; Additional file 1: Table S3). Synapse proteins were also particularly enriched (enrichment FDR: 1.90×10^{-3}).

Differences in plaque enriched proteins in EOAD and DS

Our results suggest that that major plaque enriched proteins in EOAD and DS were largely the same. The consistency of protein enrichment in plaques was even noted at an individual case level (Fig. 4C, D). However, we were interested to determine whether there was evidence of plaque protein enrichment that was unique to either DS or EOAD beyond these common plaque-enriched proteins. 20 proteins were uniquely enriched in plaques in EOAD (Additional file 1: Table S4) and 59 proteins were uniquely enriched in plaques in DS (Additional file 1: Table S5). Pathway analysis of proteins that were uniquely enriched in plaques in either DS or EOAD showed that these proteins were also enriched in endosomal or lysosomal proteins, similar to the commonly enriched plaque proteins. These protein differences between DS and EOAD did not suggest the presence of unique disease mechanisms driving plaque development in DS or EOAD: pathway analysis showed that these proteins did not cluster to a particular functional pathway and the majority of proteins showed the same trend for enrichment in plaques in the other group. 80% (63/79 proteins) of proteins uniquely enriched in plaques in either EOAD or DS were still increased in plaques in the other subtype of AD, albeit at a level that did not meet our criteria for 'enrichment in plaques'. Therefore, these results suggest that largely the same proteins are enriched in amyloid plaques in EOAD and DS.

We also directly compared plaque protein levels in DS and EOAD. For this analysis, plaque protein levels that were normalized against background protein levels for

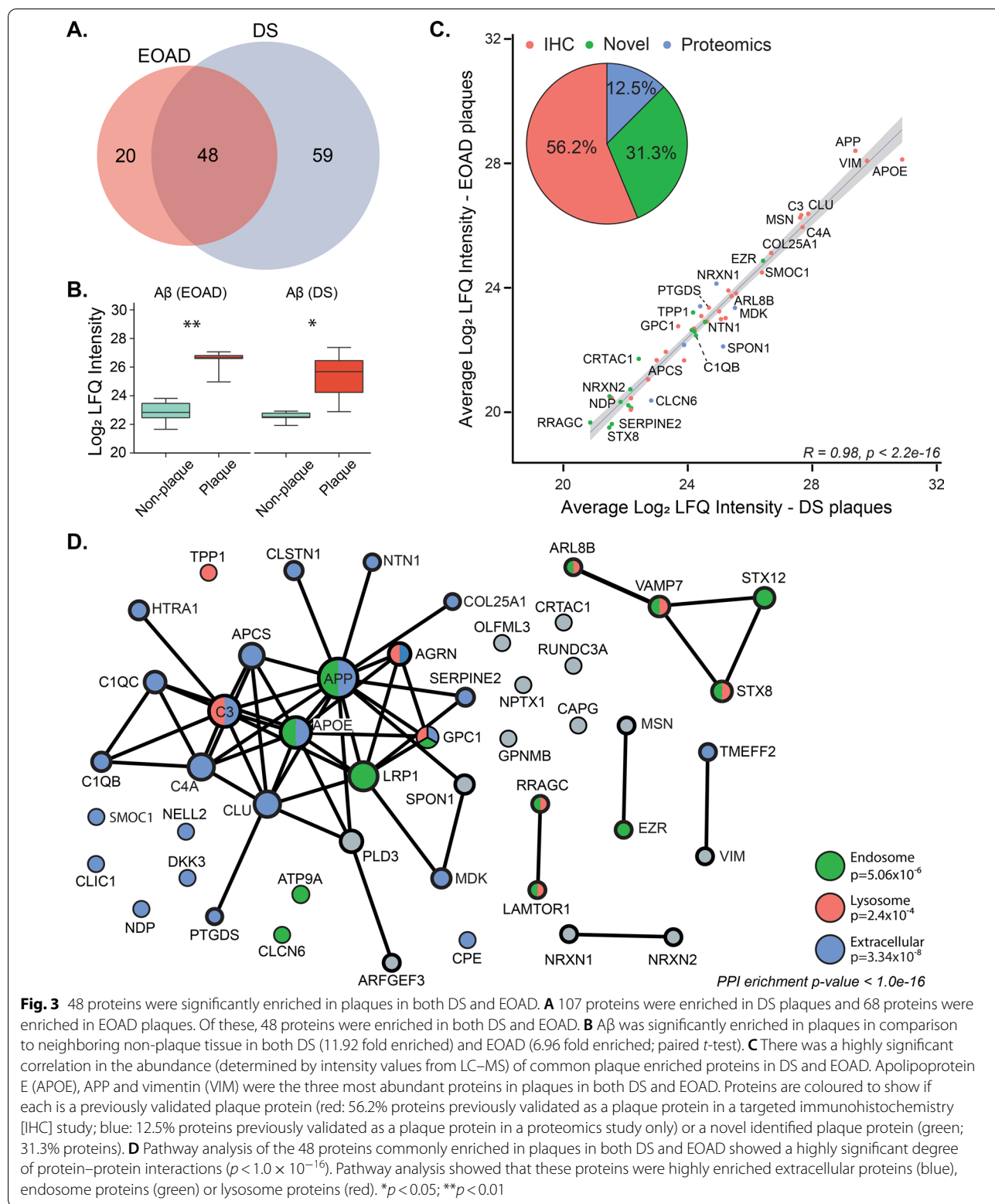
Table 2 48 proteins consistently enriched in plaques in EOAD and DS

Uniprot	Gene	Protein	Enrichment in EOAD plaques (fold change)	Enrichment in DS plaques (fold change)	Known plaque protein?	Difference in AD brain tissue	Mediates A β pathology?
Previously confirmed plaque proteins—immunohistochemistry							
Q9BX50	COL25A1	Collagen alpha-1	104.3	113.1	Yes [74]	Increased	Increases pathology [6, 75]
O95631	NTN1	Netrin-1	34.9	58.7	Yes [60]	Increased	Decreases pathology [76]
P21741	MDK	Midkine	31.4	70.4	Yes [77]	Increased	Decreases pathology [78]
Q92743	HTRA1	Serine protease HTRA1	19.0	42.8	Yes [79]	Increased	Decreases pathology [80]
Q9H4F8	SMOC1	SPARC-related modular calcium-binding protein 1	12.9	58.8	Yes [60]	Increased	Unknown
P02649	APOE	Apolipoprotein E	10.4	17.2	Yes [81]	Increased	Increases pathology [82, 83]
Q14956	GNPMB	Transmembrane glycoprotein NMB	7.8	17.8	Yes (in plaque-associated microglia) [84]	Increased	Unknown
P0C0L4	C4A	Complement C4-A	7.5	10.1	Yes [85]	Increased	Unknown
P35052	GPC1	Glypican-1	7.5	8.5	Yes [86]	Decreased	Increases pathology [87]
P02743	APCS	Serum amyloid P-component	4.9	10.8	Yes [88]	Increased	Increases pathology [89]
Q9UIK5	TMEFF2	Tomoregulin-2	4.8	6.9	Yes [90]	N/a	Decreases pathology [91]
P02746	C1QB	Complement C1q subcomponent subunit B	3.3	4.3	Yes [92]	N/a	Increases pathology [93, 94]
P10909	CLU	Clusterin	3.2	4.0	Yes [95]	Increased	Increases pathology [7, 96]
Q00604	NDP	Norrin	2.9	4.6	Yes [79]	Increased	Unknown
P05067	APP	Amyloid-beta precursor protein	2.8	5.9	Yes [97]	Increased	Increases pathology [98]
P02747	C1QC	Complement C1q subcomponent subunit C	2.7	8.4	Yes [92]	Increased	Increases pathology [93, 94]
P01024	C3	Complement C3	2.5	2.9	Yes [92]	Increased	Increases pathology [94, 99, 100]
P41222	PTGDS	Prostaglandin-H2 D-isomerase	2.2	3.0	Yes [101]	Increased	Decreases pathology [101]
P26038	MSN	Moesin	2.1	2.6	Yes, in plaque-associated microglia [102]	Increased	Decreases pathology [103]
P07093	SERPINE2	Glia-derived nexin	2.1	4.3	Yes [104]	Decreased	Increases pathology [105, 106]
Q9UBP4	DKK3	Dickkopf-related protein 3	2.1	1.8	Yes [107]	Increased	Decreases pathology [108]
Q8IV08	PLD3	Phospholipase D3	2.0	2.0	Yes [109]	N/a	Decreases pathology [110, 111]
O00468	AGRN	Agrin	1.9	2.9	Yes [112]	Increased	Decreases pathology [113]
Q07954	LRP1	Pro-low-density lipoprotein receptor-related protein 1	1.8	2.1	Yes [114]	Increased	Inconsistent effects on pathology [115]
P08670	VIM	Vimentin	1.7	1.8	Yes, in surrounding astrocytes [116]	Increased	Increases pathology [117]

Table 2 (continued)

Uniprot	Gene	Protein	Enrichment in EOAD plaques (fold change)	Enrichment in DS plaques (fold change)	Known plaque protein?	Difference in AD brain tissue	Mediates A β pathology?
P16870	CPE	Carboxypeptidase E	1.6	2.1	Yes [118]	Increased	Unknown
Q15818	NPTX1	Neuronal pentraxin-1	1.6	1.7	Yes [119]	Increased	Increases pathology [120]
Previously confirmed plaque protein—proteomics							
Q9NRN5	OLFML3	Olfactomedin-like protein 3	19.2	18.9	Yes [44]	Increased	Unknown
Q9HCB6	SPON1	Spondin-1	6.9	16.5	Yes [44]	N/a	Decreases pathology [121, 122]
O94985	CLSTN1	Calsyntenin-1	5.4	8.1	Yes [44]	Decreased	Increases pathology [123]
Q9ULB1	NRXN1	Neurexin-1	2.9	2.8	Yes [44]	Increased	Unknown
P51797	CLCN6	Chloride transport protein 6	2.8	9.7	Yes [44]	Increased	Unknown
Q9NVJ2	ARL8B	ADP-ribosylation factor-like protein 8B	2.2	2.9	Yes [44]	Increased	Decreases pathology [124]
Novel plaque proteins—mechanistic link with A β or APP							
O75110	ATP9A	Probable phospholipid-transporting ATPase IIA	1.8	2.3	No, but associated with A β [125]	Increased	Increases pathology [125]
P15311	EZR	Ezrin	1.7	2.6	No, but associated with APP [103]	Increased	Decreases pathology [103]
O00299	CLIC1	Chloride intracellular channel protein 1	1.6	1.7	No, but associated with A β [126]	Increased	Increases pathology [126]
O14773	TPP1	Tripeptidyl-peptidase 1	1.6	2.1	No, but associated with A β [127]	Increased	Decreases pathology [127]
Novel plaque proteins—no previous association with A β or APP							
P51809	VAMP7	Vesicle-associated membrane protein 7	3.0	4.0	No	N/a	Unknown
Q9UNK0	STX8	Syntaxin-8	3.2	2.4	No	Increased	Unknown
Q5TH69	ARFGEF3	Brefeldin A-inhibited guanine nucleotide-exchange protein 3	3.2	5.2	No	Increased	Unknown
Q6IAA8	LAMTOR1	Ragulator complex protein LAMTOR1	2.6	2.9	No	N/a	Unknown
Q59EK9	RUNDC3A	RUN domain-containing protein 3A	2.3	5.6	No	N/a	Unknown
P40121	CAPG	Macrophage-capping protein	2.2	1.9	No	Increased	Unknown
Q9NQ79	CRTAC1	Cartilage acidic protein 1	2.1	2.2	No	N/a	Unknown
Q9P2S2	NRXN2	Neurexin-2	1.9	2.5	No	N/a	Unknown
Q99435	NELL2	Protein kinase C-binding protein NELL2	1.8	3.9	No	N/a	Unknown
Q9HB90	RRAGC	Ras-related GTP-binding protein C	1.9	2.2	No	N/a	Unknown
Q86Y82	STX12	Syntaxin-12	1.5	2.0	No	N/a	Unknown

Proteins listed in order of fold change enrichment in EOAD; separated into previously confirmed plaque proteins, associated with A β or APP, and novel. "Previously confirmed plaque proteins" were determined by published immunohistochemistry evidence of protein presence in plaque or by > 1.5 fold enrichment in plaque in comparison to neighboring non-plaque tissue in late onset AD or preclinical AD [44]. Difference in AD tissue was determined by comparison with 33 previous proteomic studies of human AD brain tissue. "Mediates A β pathology?" determined by literature searches for "Alzheimer's disease and gene ID or protein name". Protein was designated as mediating A β pathology if altering protein expression in transgenic animal models or cell culture affected amyloid pathology



each individual case were used. 38 proteins were significantly different between DS and EOAD plaques after correction for background protein differences. 25 proteins were significantly higher and 13 proteins were significantly lower in DS plaques in comparison to EOAD plaques (Additional file 1: Table S7). Pathway analysis did not highlight enrichment of any cellular compartments or pathways for significantly different proteins in DS and EOAD plaques. Again, suggesting that plaque protein composition was largely the same in DS and EOAD.

We also examined if the triplication of chromosome 21 in DS resulted in any major differences in plaque associated proteins. Our proteomic analysis identified 22 proteins with genes on chromosome 21 (Additional file 1: Table S6). Of these, only three proteins were enriched in plaques in DS: APP, ITGB2 and COL18A1. APP was commonly enriched in plaques in both EOAD and DS. While ITGB2 and COL18A1 both had higher levels in plaques in comparison to non-plaques in EOAD, their level did not meet our criteria for designation as “enriched”. Therefore, our results suggest that the triplication of chromosome 21 is not necessarily associated with enrichment of those gene products in plaques, but rather may enhance the enrichment of selected proteins in plaques.

Validation: comparison with previous proteomic studies

Only one prior study has examined the proteome of amyloid plaques in comparison to surrounding non-plaque tissue [44]. This study identified proteins that were enriched in amyloid plaques in late-onset AD and preclinical AD. Despite the power of their dataset being limited by a small sample size ($n=3$ cases/group, pooled prior to mass spectrometry) and the different subtypes of AD analyzed in their study in comparison to ours, we were pleased to see that many of our plaque enriched proteins were validated in this previous study. 43 proteins were identified in both our study and enriched in late-onset AD plaques in Xiong et al. 26/43 commonly identified proteins were significantly enriched in either DS or EOAD plaques (Additional file 1: Table S1). The majority of the remaining proteins were also increased in plaques in our study, however they did not reach the criteria for significance in our study. All of the top 10 most highly enriched proteins in plaques in DS and EOAD in

our study were also enriched in plaques in late onset AD (Fig. 5).

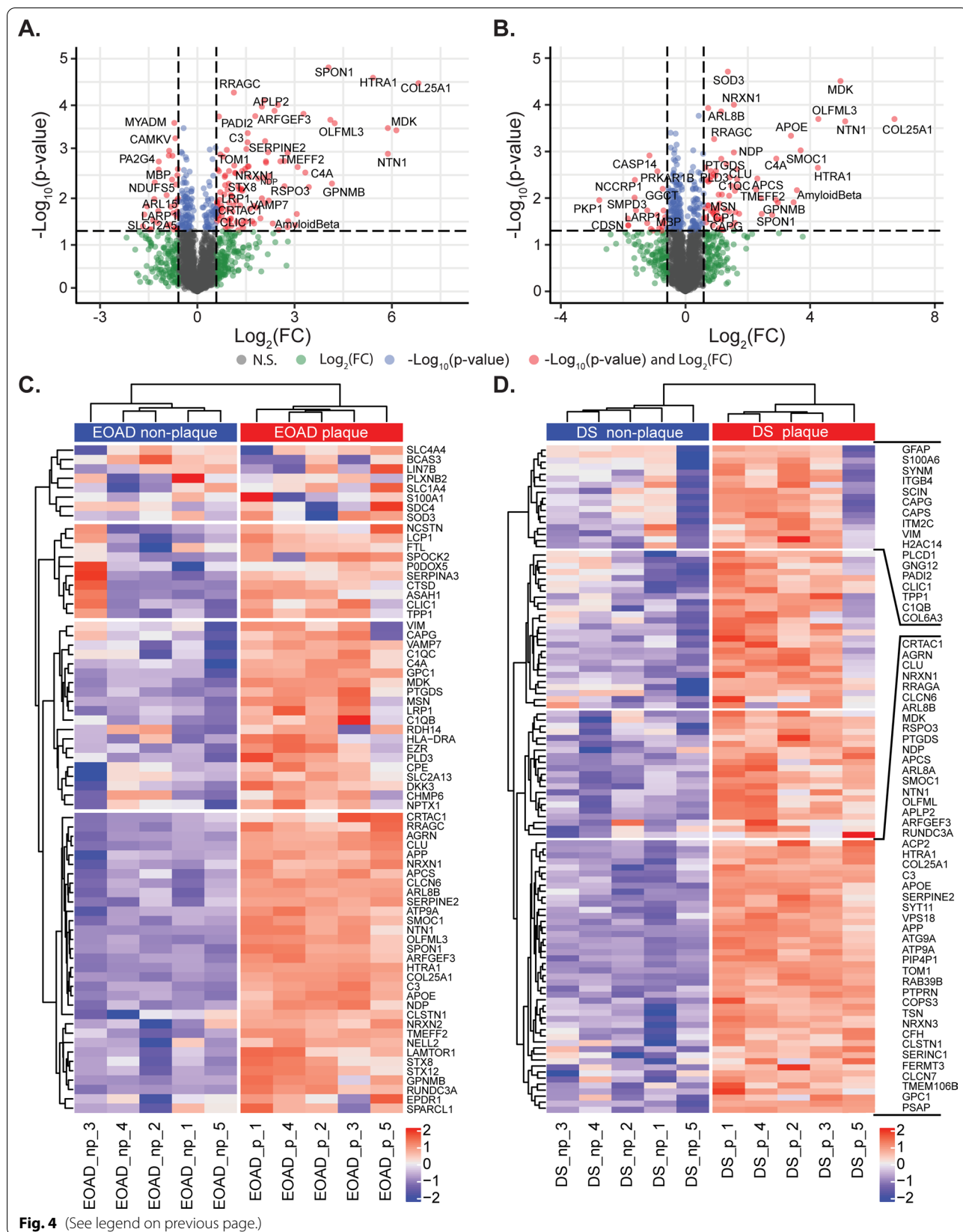
Xiong et al. also identified 78 proteins that were enriched in plaques in preclinical AD. 53 of these proteins were also identified in our study, of which, 30 were enriched in DS or EOAD plaques (Additional file 1: Table S1). The most notable protein that was not enriched in preclinical AD plaques was COL25A1, which was the most highly enriched protein in both DS and EOAD plaques in our study and was enriched in late-onset AD plaques in Xiong et al. [44]. This suggests that COL25A1 may only become enriched in plaques at a later stage of disease development. In contrast, the remaining top 10 most enriched proteins for both DS and EOAD were also enriched in plaques in preclinical AD (Fig. 5), suggesting that plaques in preclinical AD largely contain the same proteins present in plaques at advanced stages of AD.

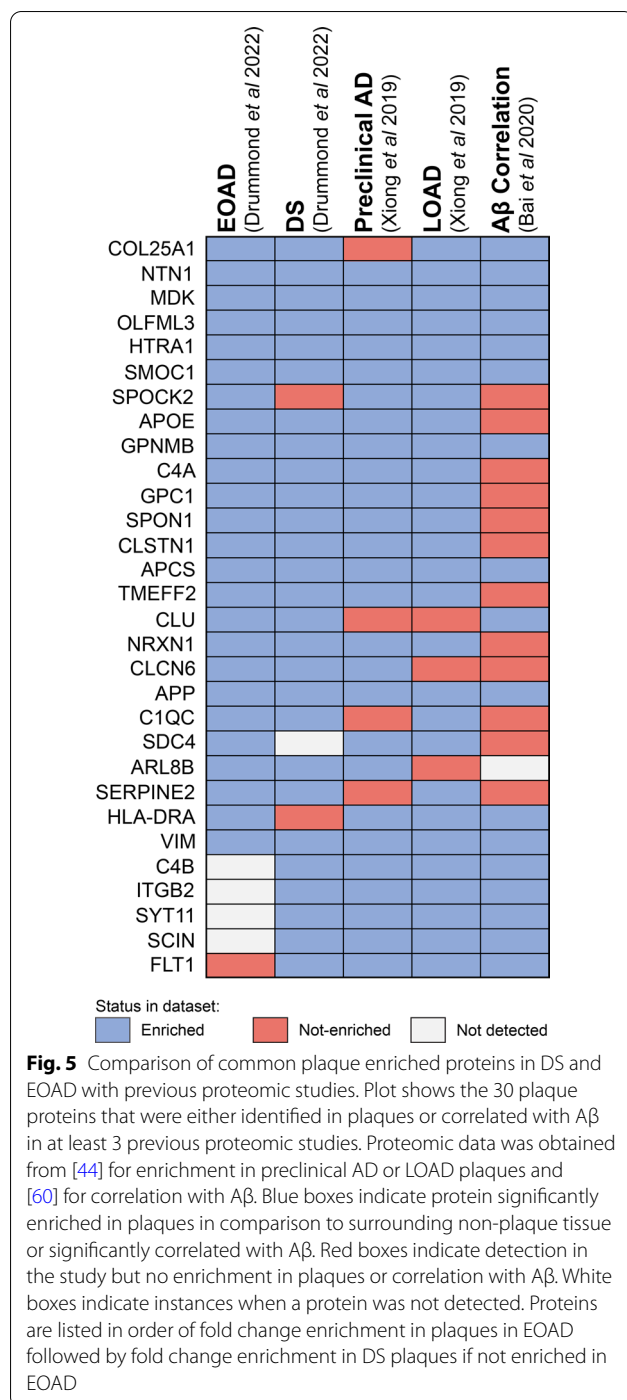
We also compared our data to Bai et al. [60] who identified 28 proteins that correlated with A β abundance in human brain tissue throughout the progression of AD. 20 of these proteins were also identified in our study, of which 13 were significantly enriched in DS and/or EOAD plaques (Additional file 1: Table S1). The remaining 7 proteins were also increased in DS and/or EOAD plaques, however these did not reach our statistical stringency level to be considered a plaque-enriched protein.

The combined analysis of our data with these two previous studies identified 30 proteins that were consistently enriched in plaques or correlated with A β in at least 3 analyses (Fig. 5). This group of proteins represent a consistent amyloid plaque signature highlighting proteins that likely have an important role in amyloid plaque pathology in addition to A β . While the some of these proteins are well known plaque proteins (e.g. APP, ApoE, clusterin), the role of many of these proteins in AD is comparatively much less studied including 8 proteins that have only been discovered as an amyloid plaque protein in proteomic studies (OLFML3, SPON1, CLSTN1, NRXN1, CLCN6, ARL8B, SYT11, SCIN). Combined, these comparisons with previous studies validates our findings and provides additional evidence that amyloid plaques are enriched in many proteins in addition to A β , many of which are likely to be of pathological importance in AD and merit further investigation.

(See figure on next page.)

Fig. 4 Significantly altered proteins in plaques in comparison to neighboring non-plaque tissue. **A, B** Volcano plots highlight proteins in red that were significantly altered in plaques in comparison to non-plaque tissue. Significance was determined by a combination of $p < 0.05$ and a fold change difference of greater than 1.5 fold. Proteins that have a fold change difference of greater than 1.5 fold only are shown in green and proteins that had a difference of $p < 0.05$ only are shown in blue. The total number of proteins included in the analysis was 2059 proteins for DS and 2115 proteins for EOAD. Proteins are identified by gene IDs. **C, D** Unsupervised clustering heatmaps for proteins that were significantly altered in DS or EOAD. Plaque and non-plaque samples independently clustered, highlighting the significantly different protein expression between plaque and non-plaque samples for DS and EOAD. All gene IDs are indicated for EOAD in each row whilst only genes from cluster 1 and 4 are marked for DS, constituting a divergent cluster and highly enriched cluster of genes respectively for DS plaques





Validation: immunohistochemistry

Fluorescent immunohistochemistry was used to validate the enrichment of four proteins in amyloid plaques. Ezrin (EZR) was selected as it was the most abundant novel plaque protein identified in our study. ARL8B was selected as a representative plaque-enriched lysosomal protein that had no prior immunohistochemistry

evidence of presence in amyloid plaques. Moesin (MSN) and SMOC1 were selected as both have only one prior publication confirming their presence in plaques using immunohistochemistry, but no immunohistochemistry evidence of enrichment in plaques in EOAD or DS. Fluorescent immunohistochemistry confirmed that ezrin, moesin, ARL8B and SMOC1 were enriched in amyloid plaques in comparison to surrounding non-plaque tissue in DS, EOAD and late-onset sporadic AD. Moesin (Fig. 6), Ezrin (Fig. 7), and SMOC1 (Fig. 8) strongly colocalized with Aβ in amyloid plaques. Particularly intense immunoreactivity was observed in the aggregated core of dense-cored plaques for these proteins. Moesin was also observed in cells with a microglial morphology in both AD and control cases, consistent with a previous study that confirmed that moesin is a microglial protein [102].

SMOC1 strongly co-localized with amyloid fibrils only in a subset of amyloid plaques (Fig. 8). The proportion of SMOC1 immunoreactive plaques in the hippocampus varied between subtypes of AD; SMOC1 was present in 58% amyloid plaques in DS in comparison to 47% of plaques in EOAD and 32% of plaques in late-onset AD (Fig. 8A, B). This was consistent with our proteomic results that found a greater enrichment of SMOC1 in DS plaques in comparison to EOAD plaques. Both neuritic and diffuse plaques showed SMOC1 immunoreactivity (Fig. 8C). Qualitatively, the proportion of SMOC1 immunoreactive plaques was higher in the hippocampus than in the neighboring cortex in all subtypes of AD. Interestingly, there was a large amount of colocalization of SMOC1 with plaques that also contained post-translationally modified Aβ species (white arrows, Fig. 8D). Minimal basal SMOC1 staining was observed in age-matched control cases, with the most consistent basal SMOC1 expression present in localized pockets of the choroid plexus.

ARL8B was also abundant in amyloid plaques in all subgroups (Fig. 9). In contrast to SMOC1, the proportion of ARL8B immunoreactive plaques in the hippocampus was similar in DS and EOAD (77% and 79%, respectively; Fig. 9A, B). However, a significantly lower proportion of plaques contained ARL8B in late-onset AD in comparison to EOAD (Fig. 9A, B). Two distinct patterns of plaque-associated ARL8B staining were observed. In one subset of amyloid plaques, bright puncta of ARL8B were diffusely present throughout plaques (Fig. 9C). In these plaques, ARL8B did not strongly colocalize with Aβ. Instead, ARL8B was often observed in the regions of amyloid plaques that were not brightly stained for Aβ (Fig. 9C). Qualitatively, ARL8B colocalization in amyloid plaques was more commonly observed in the hippocampus than the cortex. Basal ARL8B staining in control hippocampal sections was observed in neuron

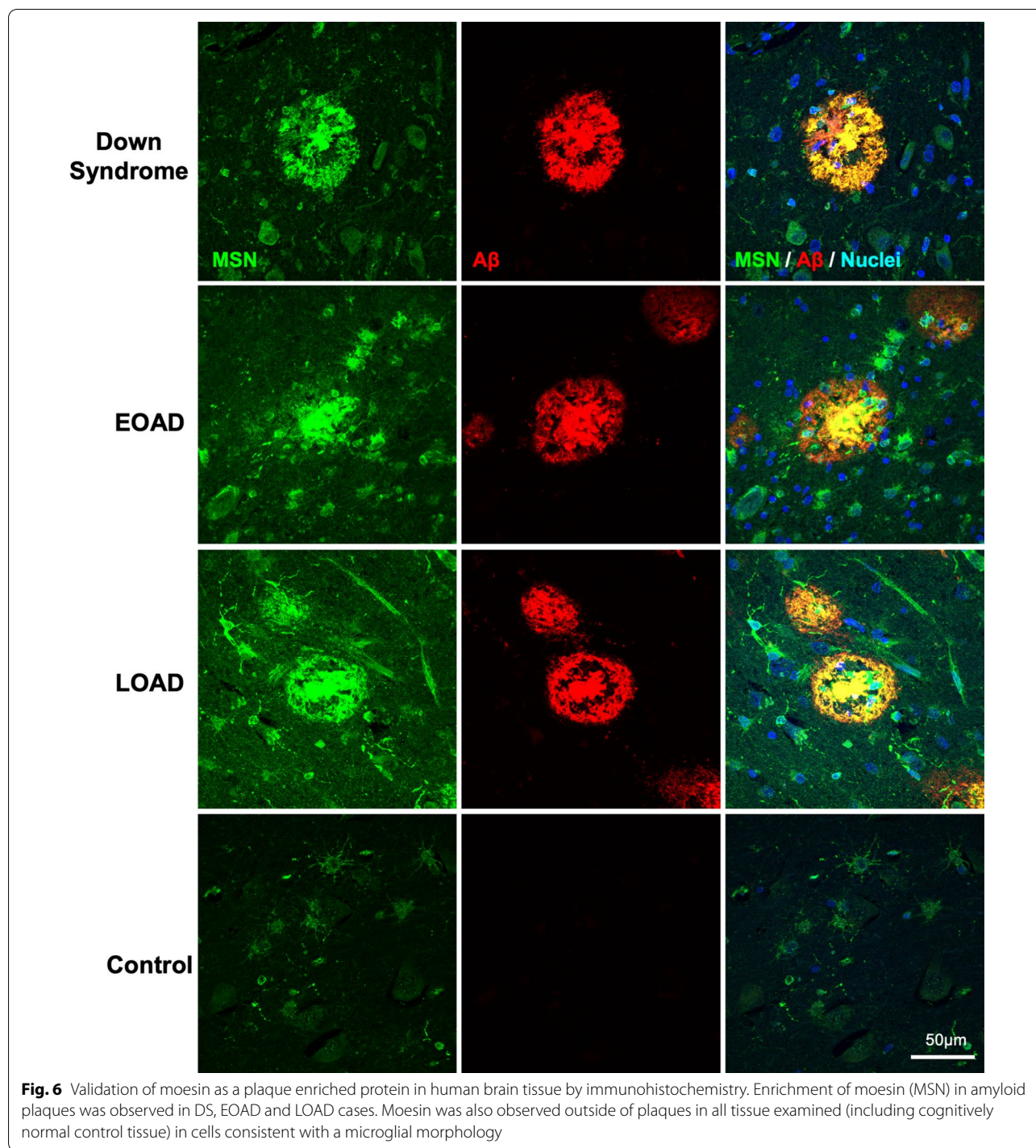


Fig. 6 Validation of moesin as a plaque enriched protein in human brain tissue by immunohistochemistry. Enrichment of moesin (MSN) in amyloid plaques was observed in DS, EOAD and LOAD cases. Moesin was also observed outside of plaques in all tissue examined (including cognitively normal control tissue) in cells consistent with a microglial morphology

soma throughout the cytoplasm and occasionally in primary processes (Fig. 9C). Staining was particularly bright in hippocampal pyramidal neurons. Abundant ARL8B was also observed in granule cells in the dentate gyrus, in the choroid plexus, and in the nucleus of some cells in white matter. The same pattern of basal staining was

observed in controls and all subtypes of AD. In the second subset of amyloid plaques, intense ARL8B immunoreactivity was observed in specific plaque-associated cells (Fig. 9D). These cells were located at the periphery of plaques and had bright, punctate ARL8B throughout the cell cytoplasm and primary processes (Fig. 9D) and

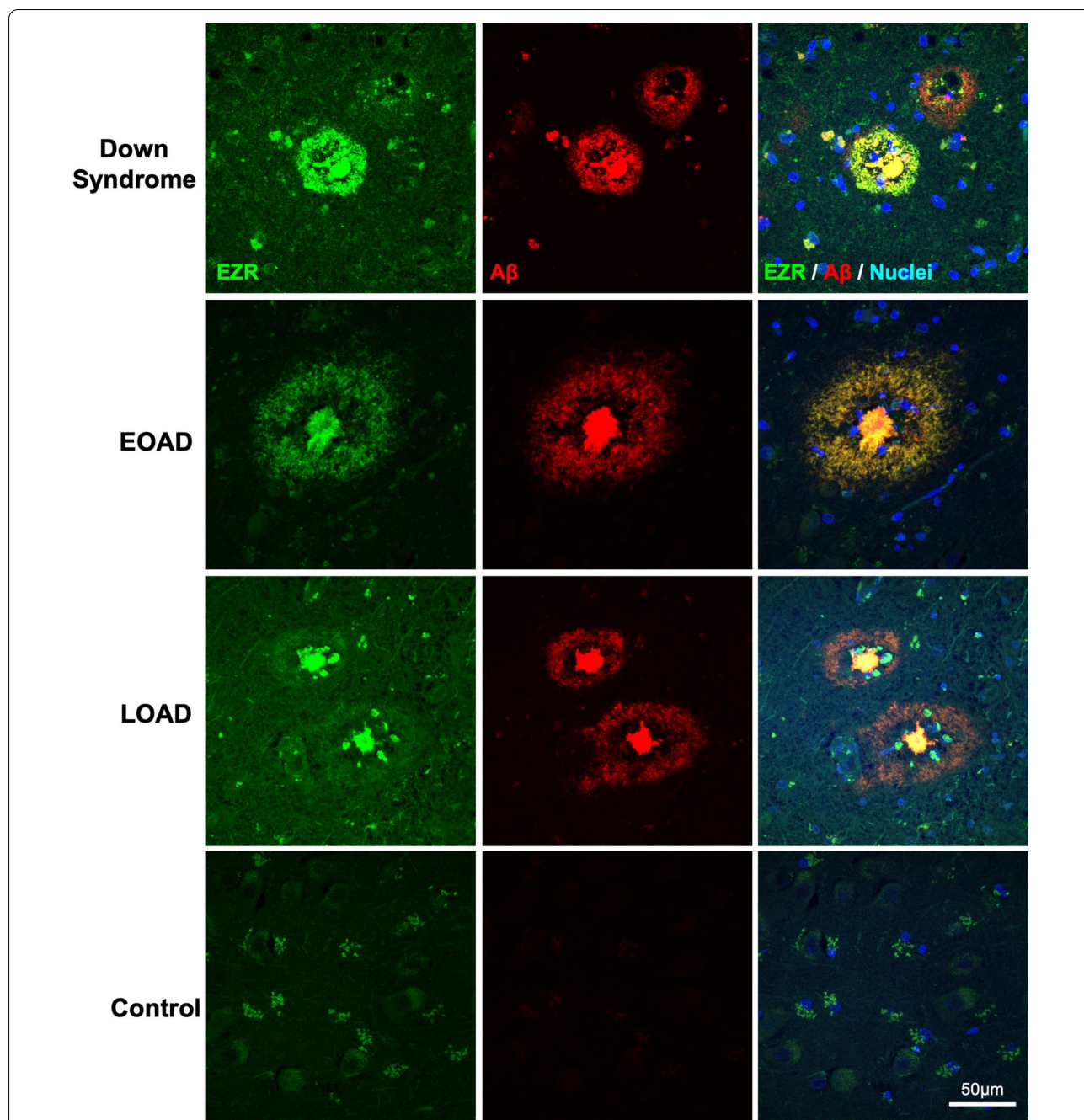
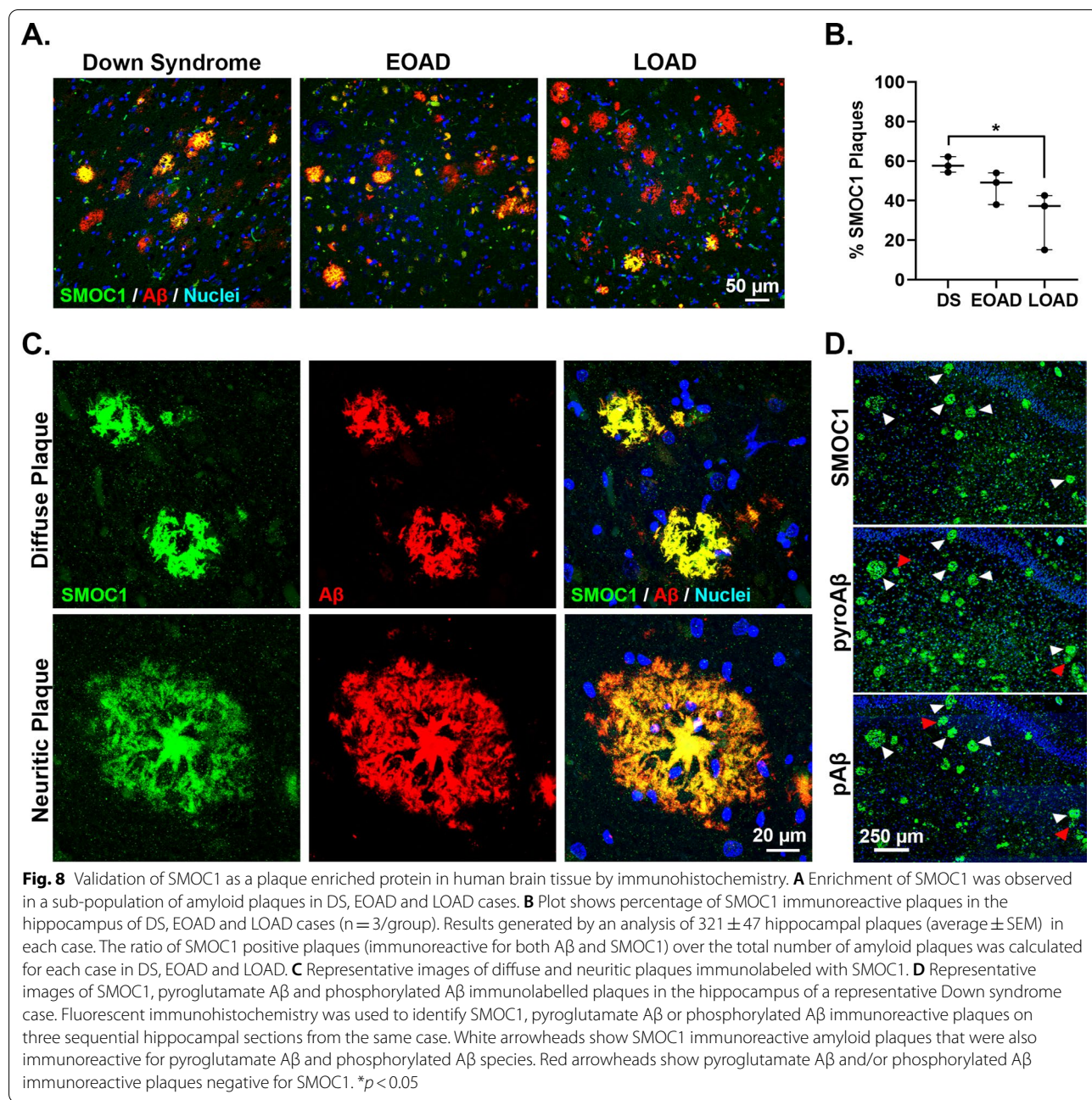


Fig. 7 Validation of ezrin as a plaque enriched protein in human brain tissue by immunohistochemistry. Enrichment of ezrin (EZR) was observed in amyloid plaques in DS, EOAD and LOAD cases

had morphology consistent with reactive glia. Double fluorescent immunohistochemistry against ARL8B and MAP2, IBA1, or GFAP showed that these ARL8B positive plaque-associated cells were a subset of reactive plaque associated astrocytes.

We also validated the presence or absence of these four plaque proteins in vascular amyloid pathology.

MSN, EZR and SMOC1 immunoreactivity occasionally co-localized with CAA or in plaques which were in direct contact with blood vessels. However, ARL8B immunoreactivity was absent in vascular amyloid pathology, which is consistent with its weak direct colocalization with Aβ in amyloid plaques (Fig. 10).

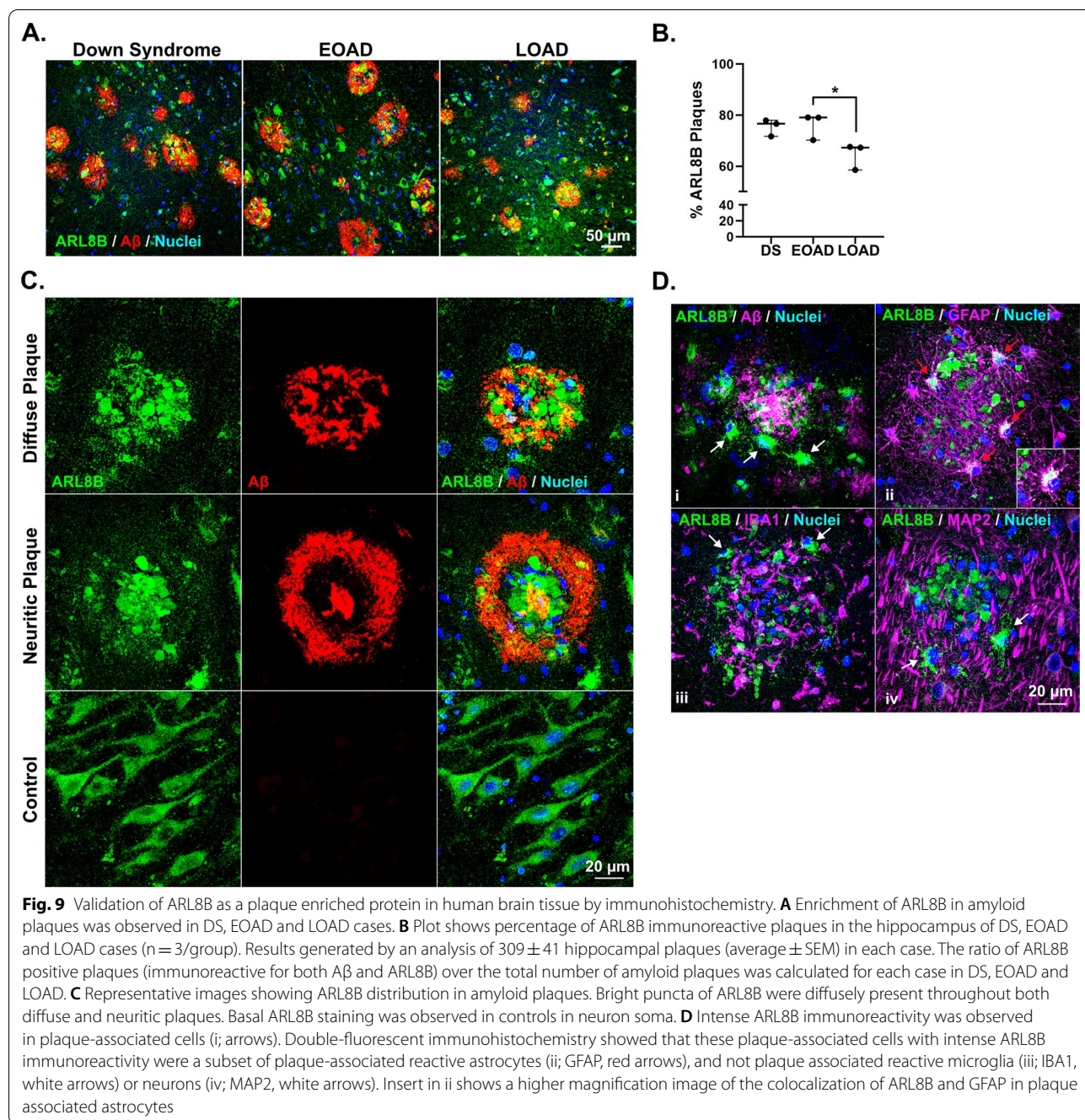


Discussion

Our results show that amyloid plaques in DS and EOAD are highly enriched in many proteins in addition to Aβ. Here, we have identified a core group of 48 proteins that are consistently enriched in plaques in comparison to neighboring non-plaque tissue in DS and EOAD. Many of these enriched plaque proteins have been validated in previous studies to colocalize with plaques or correlate with Aβ pathology in typical late onset AD, suggesting that this core group of enriched plaque proteins is consistent in both early and late onset AD subtypes. We

also identified 15 novel proteins that were consistently enriched in plaques in both DS and EOAD. Our immunohistochemistry studies showed that while similar proteins are present in plaques in DS and EOAD the relative abundance of some of these proteins (e.g. pyroglutamate Aβ, phosphorylated Aβ, SMOC1) is distinct in plaques in DS and EOAD.

Our unbiased proteomics approach highlighted the striking enrichment of many proteins in amyloid plaques that have not been extensively studied in the context of AD such as COL25A1, SMOC1, NTN1,



MDK, OLFML3 and HTRA1. The small number of previous studies examining the role of these proteins in AD suggest that these proteins likely have an important role in AD pathology. All of these highly enriched plaque proteins were also enriched in amyloid plaques in typical late onset AD [44] and 5/6 of these proteins were enriched in plaques in preclinical stages of AD [44], suggesting a possible role in the development of early AD pathology. Proteomic studies of human

AD brain bulk tissue homogenate showed that all 6 highly enriched plaque proteins were increased in AD brain tissue in multiple brain regions in comparison to age-matched cognitively normal control brain tissue [53–55, 57, 62, 128]. Prior studies have shown that COL25A1 expression increases Aβ pathology, while NTN1, MDK and HTRA1 decreases Aβ pathology in either mouse models or cell models of AD [75, 76, 80, 129], therefore showing that these proteins have an

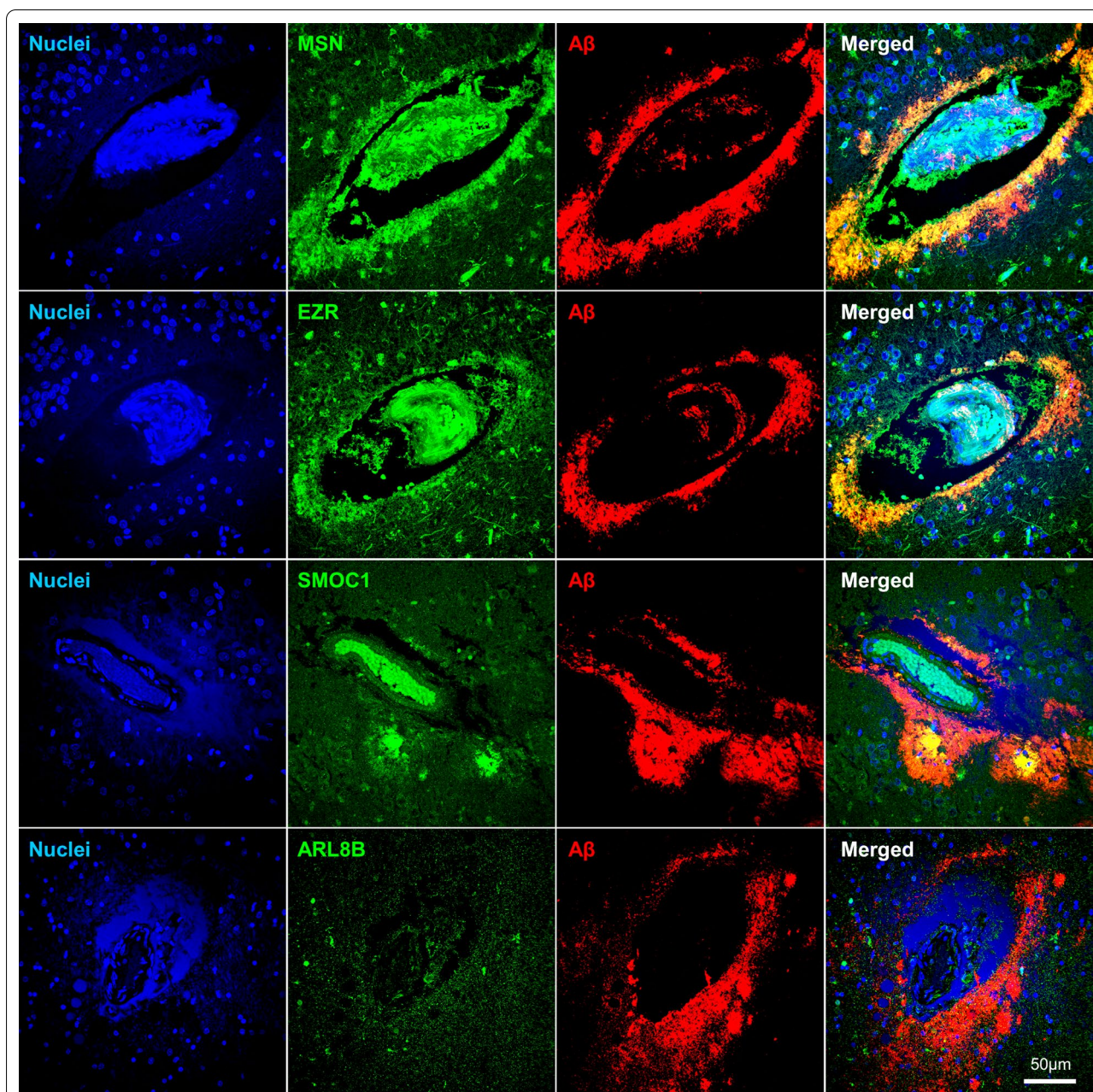


Fig. 10 Co-localization of plaque enriched proteins with vascular amyloid deposition. Representative images of vascular amyloid pathology immunolabeled with moesin (MSN), ezrin (EZR), SMOC1, ARL8B (green) and A β (4G8/6E10, red). Moesin, ezrin and SMOC1 co-localized with vascular amyloid pathology while ARL8B did not

important mechanistic role in AD. All of these major enriched plaque proteins tightly correlate with A β levels in the brain [60] and SMOC1, OLFML3, NTN1 were recently identified as novel CSF biomarkers for AD [62, 128]. Together, these results show that these major enriched amyloid plaque proteins have excellent potential as novel drug targets and/or biomarkers for AD, and should be the focus of future studies.

One of these highly enriched plaque proteins—SMOC1—was the focus of our immunohistochemistry validation studies. The role of SMOC1 in AD and its function in the brain is currently unknown. Single cell RNAseq studies suggest that SMOC1 is enriched in oligodendrocyte precursor cells in the brain [130] and previous studies have highlighted its role in glucose homeostasis [131], angiogenesis [132] and ocular and

limb development [133]. Here we show for the first time that it is highly enriched in a subpopulation of amyloid plaques. It is not yet known why SMOC1 co-localizes only with some plaques, but this could be due to SMOC1 interacting with a particular A β species such as pyroglutamate or phosphorylated A β . Indeed, our findings suggest that a large amount of SMOC1 immunoreactive amyloid plaques present in the hippocampus also contained post-translationally modified A β species. A hierarchical occurrence of A β 1–40/42, pyroglutamate and pA β throughout the course of AD has been proposed, suggesting that detection of pyroglutamate A β in amyloid plaques starts in preclinical AD, while phosphorylated A β preferentially starts aggregating in symptomatic AD [134]. Combined with our results, this might suggest that SMOC1 aggregation starts early in plaque development. A more comprehensive study looking at SMOC1 immunoreactivity in these plaque subtypes at different disease stages would provide a more definite answer. Together, our results provide further support for the important role of SMOC1 in AD and highlights the need for future studies to examine its mechanistic role in AD, particularly given the elevation of SMOC1 in the brain in preclinical AD [54]. Importantly, the finding that SMOC1 is not enriched in all plaques highlights the fact that not all amyloid plaques contain the same protein composition, which is consistent with our previous finding that plaques in rapidly progressive AD have a significantly different plaque protein expression than typical late onset AD [11].

We hypothesize that the proteins that are highly enriched in amyloid plaques have an important mechanistic role in AD pathology. A common criticism regarding the pathological importance of proteins that accumulate in plaques is that they may not have a mechanistic role in driving pathology and are simply present in plaques by chance. However, a comprehensive review of the literature does not support this criticism. 60% of the 48 proteins commonly enriched in plaques in EOAD and DS have already been confirmed to have a mechanistic role in driving AD pathology in transgenic mouse models or in vitro (Table 2). Previous studies show that 15 plaque enriched proteins pathologically promote A β aggregation/plaque formation or enhance A β associated toxicity. Notable examples include apolipoprotein E [82, 83], clusterin [7] and complement proteins (C1QB, C1QC, C3) [94, 99]. Conversely, previous studies show that 13 proteins are protective against AD pathology and can inhibit A β aggregation/plaque formation or protect against A β associated toxicity. For many of these proteins, previous research examining their mechanistic role in AD is limited to only a small number of studies. This suggests that plaque enriched proteins are not simply “tombstone

markers” of disease, but instead can provide important insight into the factors that either drive or modulate the development of pathology in AD. Additionally, this also shows that proteins enriched in amyloid plaques are a mix of pathological and protective proteins and that enrichment in plaques does not automatically suggest a detrimental role in AD.

The core group of 48 proteins enriched in plaques in both DS and EOAD were highly enriched in extracellular proteins and endosomal-lysosomal system proteins. The enrichment of extracellular proteins is expected given the extracellular location of amyloid plaques. However, the significant enrichment of endosomal-lysosomal system proteins in plaques was intriguing. A growing body of evidence convincingly shows that A β accumulates intraneuronally within endolysosomal vesicles at early stages of AD [135, 136]. Endolysosomal vesicles provide an ideal environment for A β production and aggregation: it is the location where many of the key AD associated proteins colocalize (e.g. APP, presenilin-1), the acidic environment promotes A β aggregation and, the enclosed space promotes increased interaction and aggregation [137]. These observations have prompted the inside-out amyloid hypothesis, which proposes that the gradual accumulation of intraneuronal A β 42 aggregates result in eventual synaptic/neuronal degeneration and the release of A β 42 into the extracellular space which forms the nidus of amyloid plaques [135, 137–141]. Our finding of the enrichment of endolysosomal proteins and other selected synaptic proteins in amyloid plaques in DS and EOAD supports this hypothesis.

Arl8b (encoded by the gene ARL8B) is an example novel lysosomal protein that we identified as enriched in amyloid plaques in both DS and EOAD. Arl8 is a small GTPase located on lysosomes that facilitates lysosomal trafficking along axons by acting as the linking molecule between lysosomes and kinesin-1 [142, 143]. Disruption of Arl8 function contributes to impaired lysosomal transport in axons, autophagic stress and neuron death in the neurodegenerative lysosomal storage disorder Niemann-Pick disease type C [144], confirming that it can contribute to neurodegenerative disease. The role of Arl8 in AD has not yet been studied and it has only been linked to AD in bulk-tissue ‘omics studies [54, 59]. Arl8a, the other paralog of arl8 in vertebrates, was also enriched in amyloid plaques in DS and showed a strong trend for enrichment in plaques in EOAD. Our finding that arl8b, as well as other endosomal-lysosomal proteins, were enriched in amyloid plaques provides additional support for the potential importance of lysosomes in the formation of amyloid plaques.

Our immunohistochemistry and literature validation studies showed that amyloid plaque enriched proteins had

different colocalization patterns in amyloid plaques. For example, endolysosomal proteins typically have punctate/granular localization in plaques. This staining pattern was observed for ARL8B in our study, which was identical to the staining pattern seen for other lysosomal proteins in past studies such as cathepsin D [145], cathepsin B [146], LAMP1 [147], and lipofuscin [145], which is an accumulation of highly oxidized cross-linked molecules that accumulate in lysosomes during aging. The lack of colocalization of these lysosomal proteins with A β in plaques suggests that these lysosomal proteins may not be directly interacting with A β , but may instead be located in small pockets in amyloid plaques where A β is either not present or in the process of being degraded. In contrast, SMOC1, moesin and ezrin showed high colocalization with A β fibrils in plaques, particularly in the plaque core, suggesting that these proteins likely interact directly with A β . A similar staining pattern was also observed in past studies for other major plaque proteins such as apolipoprotein E [81] and COL25A1 [148]. These results also highlight an important limitation of our study; designation as a “plaque-enriched protein” does not imply direct interaction with A β , instead this identifies a group of proteins that are significantly enriched in plaques in comparison to non-plaque tissue. While our immunohistochemistry validation results strongly suggest that some of these novel plaque-associated proteins interact with A β , future studies are required to confirm this.

Direct comparison of the amyloid plaque proteome in EOAD and DS showed that amyloid plaques in the two subtypes of younger onset AD had a very similar plaque protein composition. This shows that despite the different disease initiating factors, the resulting amyloid plaques still largely contain the same proteins. While some proteins were enriched to a much greater extent in amyloid plaques in either DS or EOAD (e.g. SMOC1), the trend for enrichment in both subtypes was highly similar. It is still unclear how these relative plaque protein differences influence AD pathogenesis. Future mechanistic studies examining how each of these proteins influence A β aggregation or clearance are needed. Future proteomic studies examining whether these major plaque enriched proteins are also enriched in other subtypes of AD (such as late onset AD, rapidly progressive AD or familial EOAD) would also potentially provide insight into differences into the rate, topography or type of plaque pathology between these subtypes.

In conclusion, we provide a new resource for the AD field that comprehensively characterizes proteins that are enriched in amyloid plaques in multiple subtypes of AD. We propose that these consistently enriched amyloid plaque proteins provide insight into the mechanisms

driving amyloid plaque development in AD and are potentially novel drug targets and/or biomarkers for AD.

Supplementary Information

The online version contains supplementary material available at <https://doi.org/10.1186/s40478-022-01356-1>.

Additional file 1: Table S1. Total imputed dataset. **Table S2.** Unimputed data. **Table S3.** Proteins enriched in plaques in both EOAD and DS (used to generate Figs. 2 and 4). **Table S4.** Proteins uniquely enriched in plaques in EOAD. **Table S5.** Proteins uniquely enriched in DS plaques. **Table S6.** Chromosome 21 proteins identified in our proteomic analysis. **Table S7.** DS vs EOAD plaque protein differences.

Additional file 2: Figure S1. *APOE* genotyping. (A) Schematic diagram of the *APOE* genotyping methodology. Six scrolls of 8 μ m were sectioned from FFPE blocks and DNA was isolated with the automated QIA-symphony SP. An endpoint PCR was performed, samples were resolved in a 2% agarose gel and amplified DNA was purified from the gel. A second PCR with the purified DNA was performed and un-purified PCR products were sequenced to determine the *APOE* genotype. (B) Representative gel of EOAD and DS samples used for sequencing. *APOE* band is located at 348 bp. (C) Sanger sequencing chromatogram showing the nucleotides located in the single-nucleotide polymorphisms (SNPs) rs429358 and rs7412, which determine the *APOE* variant ϵ 3.

Acknowledgements

This study was supported by funding from the Bluesand Foundation and the Dementia Australia Research Foundation (ED), NIH/NIA (AG056850, AG066512 and AG060882 to TW), and funding to ForeFront, a collaborative research group dedicated to the study of frontotemporal dementia and motor neuron disease, from the National Health and Medical Research Council of Australia (NHMRC) program Grant (#1132524) to ED and TK. This study was also supported by funding from the Chatrier Fondation (GP). The mass spectrometric experiments were supported with a shared instrumentation Grant from the NIH, 1S10OD010582-01A1, for the purchase of an Orbitrap Fusion Lumos. We thank Jenny Diaz for her expert advice regarding the *APOE* genotyping of FFPE tissue samples.

Author's contributions

ED and TW wrote and edited the manuscript. ED, BU and TW designed the experiments and supervised the study. ED, GP, MMA, SN, AF, VB performed the experiments. TK performed the bioinformatics. EK performed the proteomic data analysis. All authors have read and approved the final manuscript.

Declarations

Conflict of interests

The authors declare that they have no competing interests.

Author details

¹Brain and Mind Centre and School of Medical Sciences, Faculty of Medicine and Health, University of Sydney, 94 Mallett Street, Camperdown, NSW, Australia. ²Centre for Cognitive Neurology, Department of Neurology, New York University Grossman School of Medicine, Science Building, Rm 1017, 435 East 30th Street, New York, NY 10016, USA. ³Proteomics Laboratory, Division of Advanced Research Technologies, New York University Grossman School of Medicine, New York, NY, USA. ⁴Present Address: Merck & Co., Inc, Computational & Structural Chemistry, Kenilworth, NJ, USA. ⁵Department of Biochemistry and Molecular Pharmacology, NYU Grossman School of Medicine, New York, NY, USA. ⁶Departments of Pathology and Psychiatry, Neuroscience Institute, New York University Grossman School of Medicine, New York, NY, USA.

Received: 31 January 2022 Accepted: 28 March 2022

Published online: 13 April 2022

References

- Wisniewski T, Frangione B (1992) Apolipoprotein E: a pathological chaperone protein in patients with cerebral and systemic amyloid. *Neurosci Lett* 135(2):235–238
- Grundke-Iqbal I et al (1986) Microtubule-associated protein tau. A component of Alzheimer paired helical filaments. *J Biol Chem* 261(13):6084–9
- Cras P et al (1991) Senile plaque neurites in Alzheimer disease accumulate amyloid precursor protein. *Proc Natl Acad Sci U S A* 88(17):7552–7556
- Pires G et al (2019) Secernin-1 is a novel phosphorylated tau binding protein that accumulates in Alzheimer's disease and not in other tauopathies. *Acta Neuropathol Commun* 7(1):195
- Wisniewski T, Drummond E (2020) APOE-amyloid interaction: therapeutic targets. *Neurobiol Dis* 138:104784
- Hashimoto T et al (2020) Collagenous Alzheimer amyloid plaque component impacts on the compaction of amyloid-beta plaques. *Acta Neuropathol Commun* 8(1):212
- DeMattos RB et al (2002) Clusterin promotes amyloid plaque formation and is critical for neuritic toxicity in a mouse model of Alzheimer's disease. *Proc Natl Acad Sci U S A* 99(16):10843–10848
- Keren-Shaul H et al (2017) A unique microglia type associated with restricting development of Alzheimer's disease. *Cell* 169(7):1276–1290
- Perez-Nievas BG, Serrano-Pozo A (2018) Deciphering the astrocyte reaction in Alzheimer's disease. *Front Aging Neurosci* 10:114
- Serrano-Pozo A et al (2011) Neuropathological alterations in Alzheimer disease. *Cold Spring Harb Perspect Med* 1(1):a006189
- Drummond E et al (2017) Proteomic differences in amyloid plaques in rapidly progressive and sporadic Alzheimer's disease. *Acta Neuropathol* 133(6):933–954
- Drummond E et al (2020) Phosphorylated tau interactome in the human Alzheimer's disease brain. *Brain* 143(9):2803–2817
- Drummond ES et al (2015) Proteomic analysis of neurons microdissected from formalin-fixed, paraffin-embedded Alzheimer's disease brain tissue. *Sci Rep* 5:15456
- Cohen ML et al (2015) Rapidly progressive Alzheimer's disease features distinct structures of amyloid-beta. *Brain* 138(Pt 4):1009–1022
- Murray ME et al (2011) Neuropathologically defined subtypes of Alzheimer's disease with distinct clinical characteristics: a retrospective study. *Lancet Neurol* 10(9):785–796
- Emrani S et al (2020) APOE4 is associated with cognitive and pathological heterogeneity in patients with Alzheimer's disease: a systematic review. *Alzheimers Res Ther* 12(1):141
- Neff RA et al (2021) Molecular subtyping of Alzheimer's disease using RNA sequencing data reveals novel mechanisms and targets. *Sci Adv* 7(2):eabb5398
- Reitz C, Roggeva E, Beecham GW (2020) Late-onset vs nonmendelian early-onset Alzheimer disease: a distinction without a difference? *Neurol Genet* 6(5):e512
- Ballard C et al (2016) Dementia in Down's syndrome. *Lancet Neurol* 15(6):622–636
- Teller JK et al (1996) Presence of soluble amyloid beta-peptide precedes amyloid plaque formation in Down's syndrome. *Nat Med* 2(1):93–95
- Gyure KA et al (2001) Intraneuronal abeta-amyloid precedes development of amyloid plaques in Down syndrome. *Arch Pathol Lab Med* 125(4):489–492
- Mori C et al (2002) Intraneuronal Abeta42 accumulation in Down syndrome brain. *Amyloid* 9(2):88–102
- Lemere CA et al (1996) Sequence of deposition of heterogeneous amyloid beta-peptides and APO E in Down syndrome: implications for initial events in amyloid plaque formation. *Neurobiol Dis* 3(1):16–32
- Wisniewski KE, Wisniewski HM, Wen GY (1985) Occurrence of neuropathological changes and dementia of Alzheimer's disease in Down's syndrome. *Ann Neurol* 17(3):278–282
- Davidson YS et al (2018) The age of onset and evolution of Braak tangle stage and Thal amyloid pathology of Alzheimer's disease in individuals with Down syndrome. *Acta Neuropathol Commun* 6(1):56
- Cohen AD et al (2018) Early striatal amyloid deposition distinguishes Down syndrome and autosomal dominant Alzheimer's disease from late-onset amyloid deposition. *Alzheimers Dement* 14(6):743–750
- Mann DMA et al (2018) Patterns and severity of vascular amyloid in Alzheimer's disease associated with duplications and missense mutations in APP gene, Down syndrome and sporadic Alzheimer's disease. *Acta Neuropathol* 136(4):569–587
- Kumar S, Lemere CA, Walter J (2020) Phosphorylated Abeta peptides in human Down syndrome brain and different Alzheimer's-like mouse models. *Acta Neuropathol Commun* 8(1):118
- Frost JL et al (2013) Pyroglutamate-3 amyloid-beta deposition in the brains of humans, non-human primates, canines, and Alzheimer disease-like transgenic mouse models. *Am J Pathol* 183(2):369–381
- Saido TC et al (1995) Dominant and differential deposition of distinct beta-amyloid peptide species, A beta N3(pE), in senile plaques. *Neuron* 14(2):457–466
- Iwatsubo T et al (1996) Full-length amyloid-beta (1–42(43)) and amino-terminally modified and truncated amyloid-beta 42(43) deposit in diffuse plaques. *Am J Pathol* 149(6):1823–1830
- Montine TJ et al (2012) National Institute on Aging-Alzheimer's Association guidelines for the neuropathologic assessment of Alzheimer's disease: a practical approach. *Acta Neuropathol* 123(1):1–11
- Miller DL et al (2011) High-affinity rabbit monoclonal antibodies specific for amyloid peptides amyloid-beta40 and amyloid-beta42. *J Alzheimers Dis* 23(2):293–305
- Mehta PD et al (2018) Generation and partial characterization of rabbit monoclonal antibody to pyroglutamate amyloid-beta3-42 (pE3-Abeta). *J Alzheimers Dis* 62(4):1635–1649
- Herline K et al (2018) Immunotherapy to improve cognition and reduce pathological species in an Alzheimer's disease mouse model. *Alzheimers Res Ther* 10(1):54
- Drummond E et al (2018) Isolation of amyloid plaques and neurofibrillary tangles from archived Alzheimer's disease tissue using laser-capture microdissection for downstream proteomics. *Methods Mol Biol* 1723:319–334
- Drummond E et al (2017) Isolation of amyloid plaques and neurofibrillary tangles from archived Alzheimer's disease tissue using laser capture microdissection for downstream proteomics. *Methods Mol Biol* 1723:319–334
- Cox J et al (2014) Accurate proteome-wide label-free quantification by delayed normalization and maximal peptide ratio extraction, termed MaxLFQ. *Mol Cell Proteomics* 13(9):2513–2526
- Cox J et al (2011) Andromeda: a peptide search engine integrated into the MaxQuant environment. *J Proteome Res* 10(4):1794–1805
- Tyanova S et al (2016) The Perseus computational platform for comprehensive analysis of (pro)teomics data. *Nat Methods* 13(9):731–740
- Seyfried NT et al (2017) A multi-network approach identifies protein-specific co-expression in asymptomatic and symptomatic Alzheimer's disease. *Cell Syst* 4(1):60–72
- R Core Team (2020) R: a language and environment for statistical computing. R Foundation for Statistical Computing, Vienna
- Szklarczyk D et al (2020) The STRING database in 2021: customizable protein-protein networks, and functional characterization of user-uploaded gene/measurement sets. *Nucl Acids Res* 49(D1):D605–D612
- Xiong F, Ge W, Ma C (2019) Quantitative proteomics reveals distinct composition of amyloid plaques in Alzheimer's disease. *Alzheimers Dement* 15:429–440
- Liao L et al (2004) Proteomic characterization of postmortem amyloid plaques isolated by laser capture microdissection. *J Biol Chem* 279(35):37061–37068
- Musunuri S et al (2014) Quantification of the brain proteome in Alzheimer's disease using multiplexed mass spectrometry. *J Proteome Res* 13(4):2056–2068
- Andreev VP et al (2012) Label-free quantitative LC-MS proteomics of Alzheimer's disease and normally aged human brains. *J Proteome Res* 11(6):3053–3067
- Donovan LE et al (2012) Analysis of a membrane-enriched proteome from postmortem human brain tissue in Alzheimer's disease. *Proteomics Clin Appl* 6(3–4):201–211
- Manavalan A et al (2013) Brain site-specific proteome changes in aging-related dementia. *Exp Mol Med* 45:e39
- Hondius DC et al (2016) Profiling the human hippocampal proteome at all pathologic stages of Alzheimer's disease. *Alzheimers Dement* 12(6):654–668

51. Ho Kim J et al (2015) Proteome-wide characterization of signalling interactions in the hippocampal CA4/DG subfield of patients with Alzheimer's disease. *Sci Rep* 5:11138
52. Sweet RA et al (2016) Apolipoprotein E*4 (APOE*4) genotype is associated with altered levels of glutamate signaling proteins and synaptic coexpression networks in the prefrontal cortex in mild to moderate Alzheimer disease. *Mol Cell Proteomics* 15(7):2252–2262
53. Hales CM et al (2016) Changes in the detergent-insoluble brain proteome linked to amyloid and tau in Alzheimer's disease progression. *Proteomics* 16(23):3042–3053
54. Johnson ECB et al (2018) Deep proteomic network analysis of Alzheimer's disease brain reveals alterations in RNA binding proteins and RNA splicing associated with disease. *Mol Neurodegener* 13(1):52
55. Zhang Q et al (2018) Integrated proteomics and network analysis identifies protein hubs and network alterations in Alzheimer's disease. *Acta Neuropathol Commun* 6(1):19
56. Mendonca CF et al (2019) Proteomic signatures of brain regions affected by tau pathology in early and late stages of Alzheimer's disease. *Neurobiol Dis* 130:104509
57. Xu J et al (2019) Regional protein expression in human Alzheimer's brain correlates with disease severity. *Commun Biol* 2:43
58. Muraoka S et al (2020) Proteomic and biological profiling of extracellular vesicles from Alzheimer's disease human brain tissues. *Alzheimers Dement* 16:896–907
59. Johnson ECB et al (2020) Large-scale proteomic analysis of Alzheimer's disease brain and cerebrospinal fluid reveals early changes in energy metabolism associated with microglia and astrocyte activation. *Nat Med* 26(5):769–780
60. Bai B et al (2020) Deep multilayer brain proteomics identifies molecular networks in Alzheimer's disease progression. *Neuron* 105:975–991
61. Haytural H et al (2020) The proteome of the dentate terminal zone of the perforant path indicates presynaptic impairment in Alzheimer disease. *Mol Cell Proteomics* 19(1):128–141
62. Higginbotham L et al (2020) Integrated proteomics reveals brain-based cerebrospinal fluid biomarkers in asymptomatic and symptomatic Alzheimer's disease. *Sci Adv* 6(43):eaz9360
63. Stepler KE et al (2020) Inclusion of African American/Black adults in a pilot brain proteomics study of Alzheimer's disease. *Neurobiol Dis* 146:105129
64. Ping L et al (2020) Global quantitative analysis of the human brain proteome and phosphoproteome in Alzheimer's disease. *Sci Data* 7(1):315
65. Sathé G et al (2020) Quantitative proteomic analysis of the frontal cortex in Alzheimer's disease. *J Neurochem* 156:988
66. Wang Z et al (2020) 27-plex tandem mass tag mass spectrometry for profiling brain proteome in Alzheimer's disease. *Anal Chem* 92(10):7162–7170
67. Li X et al (2021) Sequence of proteome profiles in preclinical and symptomatic Alzheimer's disease. *Alzheimers Dement* 17:946–958
68. Hondius DC et al (2021) The proteome of granulovacuolar degeneration and neurofibrillary tangles in Alzheimer's disease. *Acta Neuropathol* 141:341–358
69. Wingo AP et al (2020) Shared proteomic effects of cerebral atherosclerosis and Alzheimer's disease on the human brain. *Nat Neurosci* 23(6):696–700
70. McKetney J et al (2019) Proteomic atlas of the human brain in Alzheimer's disease. *J Proteome Res* 18(3):1380–1391
71. Pearson A et al (2020) Molecular abnormalities in autopsied brain tissue from the inferior horn of the lateral ventricles of nonagenarians and Alzheimer disease patients. *BMC Neurol* 20(1):317
72. Dai J et al (2018) Effects of APOE genotype on brain proteomic network and cell type changes in Alzheimer's disease. *Front Mol Neurosci* 11:454
73. Carlyle BC et al (2021) Synaptic proteins associated with cognitive performance and neuropathology in older humans revealed by multiplexed fractionated proteomics. *Neurobiol Aging* 105:99–114
74. Hashimoto T et al (2002) CLAC: a novel Alzheimer amyloid plaque component derived from a transmembrane precursor. *CLAC-P/collagen type XXV EMBO J* 21(7):1524–1534
75. Tong Y et al (2010) COL25A1 triggers and promotes Alzheimer's disease-like pathology in vivo. *Neurogenetics* 11(1):41–52
76. Spilman PR et al (2016) Netrin-1 interrupts amyloid-beta amplification, increases sAβ₄₂ in vitro and in vivo, and improves cognition in a mouse model of Alzheimer's disease. *J Alzheimers Dis* 52(1):223–242
77. Yasuhara O et al (1993) Midkine, a novel neurotrophic factor, is present in senile plaques of Alzheimer disease. *Biochem Biophys Res Commun* 192(1):246–251
78. Muramatsu H et al (2011) Midkine as a factor to counteract the deposition of amyloid beta-peptide plaques: in vitro analysis and examination in knockout mice. *Int Arch Med* 4(1):1
79. Hondius DC et al (2018) Proteomics analysis identifies new markers associated with capillary cerebral amyloid angiopathy in Alzheimer's disease. *Acta Neuropathol Commun* 6(1):46
80. Grau S et al (2005) Implications of the serine protease HtrA1 in amyloid precursor protein processing. *Proc Natl Acad Sci U S A* 102(17):6021–6026
81. Namba Y et al (1991) Apolipoprotein E immunoreactivity in cerebral amyloid deposits and neurofibrillary tangles in Alzheimer's disease and kuru plaque amyloid in Creutzfeldt-Jakob disease. *Brain Res* 541(1):163–166
82. Bales KR et al (1997) Lack of apolipoprotein E dramatically reduces amyloid beta-peptide deposition. *Nat Genet* 17(3):263–264
83. Holtzman DM et al (2000) Apolipoprotein E isoform-dependent amyloid deposition and neuritic degeneration in a mouse model of Alzheimer's disease. *Proc Natl Acad Sci U S A* 97(6):2892–2897
84. Huttenrauch M et al (2018) Glycoprotein NMB: a novel Alzheimer's disease associated marker expressed in a subset of activated microglia. *Acta Neuropathol Commun* 6(1):108
85. Eikelenboom P, Stam FC (1984) An immunohistochemical study on cerebral vascular and senile plaque amyloid in Alzheimer's dementia. *Virchows Arch B Cell Pathol Incl Mol Pathol* 47(1):17–25
86. van Horsen J et al (2001) Heparan sulfate proteoglycan expression in cerebrovascular amyloid beta deposits in Alzheimer's disease and hereditary cerebral hemorrhage with amyloidosis (Dutch) brains. *Acta Neuropathol* 102(6):604–614
87. Watanabe N et al (2004) Glypican-1 as an Aβ binding HSPG in the human brain: its localization in DIG domains and possible roles in the pathogenesis of Alzheimer's disease. *FASEB J* 18(9):1013–1015
88. McGeer EG et al (2001) The pentraxins: possible role in Alzheimer's disease and other innate inflammatory diseases. *Neurobiol Aging* 22(6):843–848
89. Tennent GA, Lovat LB, Pepys MB (1995) Serum amyloid P component prevents proteolysis of the amyloid fibrils of Alzheimer disease and systemic amyloidosis. *Proc Natl Acad Sci U S A* 92(10):4299–4303
90. Siegel DA et al (2006) Tomoregulin-2 is found extensively in plaques in Alzheimer's disease brain. *J Neurochem* 98(1):34–44
91. Hong HS et al (2015) Tomoregulin (TMEFF2) binds Alzheimer's disease amyloid-beta (Aβ) oligomer and Aβ₄₂ and protects neurons from Aβ-induced toxicity. *J Alzheimers Dis* 48(3):731–743
92. Eikelenboom P, Stam FC (1982) Immunoglobulins and complement factors in senile plaques: an immunoperoxidase study. *Acta Neuropathol* 57(2–3):239–242
93. Fonseca MI et al (2004) Absence of C1q leads to less neuropathology in transgenic mouse models of Alzheimer's disease. *J Neurosci* 24(29):6457–6465
94. Hong S et al (2016) Complement and microglia mediate early synapse loss in Alzheimer mouse models. *Science* 352(6286):712–716
95. Choi-Miura NH et al (1992) SP-40,40 is a constituent of Alzheimer's amyloid. *Acta Neuropathol* 83(3):260–264
96. Oh SB et al (2019) Clusterin contributes to early stage of Alzheimer's disease pathogenesis. *Brain Pathol* 29(2):217–231
97. Glenner GG, Wong CW (1984) Alzheimer's disease: initial report of the purification and characterization of a novel cerebrovascular amyloid protein. *Biochem Biophys Res Commun* 120(3):885–890
98. Drummond E, Wisniewski T (2017) Alzheimer's disease: experimental models and reality. *Acta Neuropathol* 133(2):155–175
99. Shi Q et al (2017) Complement C3 deficiency protects against neurodegeneration in aged plaque-rich APP/PS1 mice. *Sci Transl Med* 9(392)
100. Wu T et al (2019) Complement C3 is activated in human AD brain and is required for neurodegeneration in mouse models of amyloidosis and tauopathy. *Cell Rep* 28(8):2111–2123
101. Kanekiyo T et al (2007) Lipocalin-type prostaglandin D synthase/β₂-microglobulin is a major amyloid beta-chaperone in human cerebrospinal fluid. *Proc Natl Acad Sci U S A* 104(15):6412–6417
102. Rayaprolu S et al (2020) Flow-cytometric microglial sorting coupled with quantitative proteomics identifies moesin as a highly-abundant microglial protein with relevance to Alzheimer's disease. *Mol Neurodegener* 15(1):28

103. Darmellah A et al (2012) Ezrin/radixin/moesin are required for the purinergic P2X7 receptor (P2X7R)-dependent processing of the amyloid precursor protein. *J Biol Chem* 287(41):34583–34595
104. Rosenblatt DE, Geula C, Mesulam MM (1989) Protease nexin I immunostaining in Alzheimer's disease. *Ann Neurol* 26(5):628–634
105. Jacobsen JS et al (2008) Enhanced clearance of Abeta in brain by sustaining the plasmin proteolysis cascade. *Proc Natl Acad Sci U S A* 105(25):8754–8759
106. Liu RM et al (2011) Knockout of plasminogen activator inhibitor 1 gene reduces amyloid beta peptide burden in a mouse model of Alzheimer's disease. *Neurobiol Aging* 32(6):1079–1089
107. Bruggink KA et al (2015) Dickkopf-related protein 3 is a potential Abeta-associated protein in Alzheimer's disease. *J Neurochem* 134(6):1152–1162
108. Zhang L et al (2017) Dickkopf 3 (Dkk3) Improves amyloid-beta pathology, cognitive dysfunction, and cerebral glucose metabolism in a transgenic mouse model of Alzheimer's disease. *J Alzheimers Dis* 60(2):733–746
109. Satoh J et al (2014) PLD3 is accumulated on neuritic plaques in Alzheimer's disease brains. *Alzheimers Res Ther* 6(9):70
110. Mukadam AS, Breusegem SY, Seaman MNJ (2018) Analysis of novel endosome-to-Golgi retrieval genes reveals a role for PLD3 in regulating endosomal protein sorting and amyloid precursor protein processing. *Cell Mol Life Sci* 75(14):2613–2625
111. Demirev AV et al (2019) V232M substitution restricts a distinct O-glycosylation of PLD3 and its neuroprotective function. *Neurobiol Dis* 129:182–194
112. Donahue JE et al (1999) Agrin in Alzheimer's disease: altered solubility and abnormal distribution within microvasculature and brain parenchyma. *Proc Natl Acad Sci U S A* 96(11):6468–6472
113. Rauch SM et al (2011) Changes in brain beta-amyloid deposition and aquaporin 4 levels in response to altered agrin expression in mice. *J Neuropathol Exp Neurol* 70(12):1124–1137
114. Rebeck GW et al (1995) Multiple, diverse senile plaque-associated proteins are ligands of an apolipoprotein E receptor, the alpha 2-macroglobulin receptor/low-density-lipoprotein receptor-related protein. *Ann Neurol* 37(2):211–217
115. Shinohara M et al (2017) Role of LRP1 in the pathogenesis of Alzheimer's disease: evidence from clinical and preclinical studies. *J Lipid Res* 58(7):1267–1281
116. Yamada T et al (1992) Vimentin immunoreactivity in normal and pathological human brain tissue. *Acta Neuropathol* 84(2):157–162
117. Kamphuis W et al (2015) GFAP and vimentin deficiency alters gene expression in astrocytes and microglia in wild-type mice and changes the transcriptional response of reactive glia in mouse model for Alzheimer's disease. *Glia* 63(6):1036–1056
118. Pla V et al (2013) Secretory sorting receptors carboxypeptidase E and secretogranin III in amyloid beta-associated neural degeneration in Alzheimer's disease. *Brain Pathol* 23(3):274–284
119. Cummings DM et al (2017) Neuronal and peripheral pentraxins modify glutamate release and may interact in blood-brain barrier failure. *Cereb Cortex* 27(6):3437–3448
120. Abad MA et al (2006) Neuronal pentraxin 1 contributes to the neuronal damage evoked by amyloid-beta and is overexpressed in dystrophic neurites in Alzheimer's brain. *J Neurosci* 26(49):12735–12747
121. Hafez DM et al (2012) F-spondin gene transfer improves memory performance and reduces amyloid-beta levels in mice. *Neuroscience* 223:465–472
122. Park SY et al (2020) SPON1 can reduce amyloid beta and reverse cognitive impairment and memory dysfunction in Alzheimer's disease mouse model. *Cells* 9(5):1275
123. Gotoh N et al (2020) Amyloidogenic processing of amyloid beta protein precursor (APP) is enhanced in the brains of alcadein alpha-deficient mice. *J Biol Chem* 295(28):9650–9662
124. Griffin EF et al (2018) Distinct functional roles of Vps41-mediated neuroprotection in Alzheimer's and Parkinson's disease models of neurodegeneration. *Hum Mol Genet* 27(24):4176–4193
125. Teranishi Y et al (2015) Proton myo-inositol cotransporter is a novel gamma-secretase associated protein that regulates Abeta production without affecting Notch cleavage. *FEBS J* 282(17):3438–3451
126. Novarino G et al (2004) Involvement of the intracellular ion channel CLIC1 in microglia-mediated beta-amyloid-induced neurotoxicity. *J Neurosci* 24(23):5322–5330
127. Sole-Domenech S et al (2018) Lysosomal enzyme tripeptidyl peptidase 1 destabilizes fibrillar Abeta by multiple endoproteolytic cleavages within the beta-sheet domain. *Proc Natl Acad Sci U S A* 115(7):1493–1498
128. Wang H et al (2020) Integrated analysis of ultra-deep proteomes in cortex, cerebrospinal fluid and serum reveals a mitochondrial signature in Alzheimer's disease. *Mol Neurodegener* 15(1):43
129. Chen G et al (2021) Netrin-1 receptor UNC5C cleavage by active delta-secretase enhances neurodegeneration, promoting Alzheimer's disease pathologies. *Sci Adv* 7(16)
130. Allen Institute for Brain Science (2019) Allen cell types database-multiple cortical areas smart-seq. https://celltypes.brain-map.org/maseq/human_ctx_smart-seq
131. Montgomery MK et al (2020) SMOC1 is a glucose-responsive hepatokine and therapeutic target for glycemic control. *Sci Transl Med* 12(559):eaaz8048
132. Awwad K et al (2015) Role of secreted modular calcium-binding protein 1 (SMOC1) in transforming growth factor beta signalling and angiogenesis. *Cardiovasc Res* 106(2):284–294
133. Okada I et al (2011) SMOC1 is essential for ocular and limb development in humans and mice. *Am J Hum Genet* 88(1):30–41
134. Rijal Upadhaya A et al (2014) Biochemical stages of amyloid-beta peptide aggregation and accumulation in the human brain and their association with symptomatic and pathologically preclinical Alzheimer's disease. *Brain* 137(Pt 3):887–903
135. Gouras GK et al (2000) Intraneuronal Abeta42 accumulation in human brain. *Am J Pathol* 156(1):15–20
136. Takahashi RH et al (2002) Intraneuronal Alzheimer abeta42 accumulates in multivesicular bodies and is associated with synaptic pathology. *Am J Pathol* 161(5):1869–1879
137. Gouras GK et al (2010) Intraneuronal beta-amyloid accumulation and synapse pathology in Alzheimer's disease. *Acta Neuropathol* 119(5):523–541
138. Gouras GK, Willen K, Faideau M (2014) The inside-out amyloid hypothesis and synapse pathology in Alzheimer's disease. *Neurodegener Dis* 13(2–3):142–146
139. D'Andrea MR et al (2001) Evidence that neurones accumulating amyloid can undergo lysis to form amyloid plaques in Alzheimer's disease. *Histopathology* 38(2):120–134
140. Pensalfini A et al (2014) Intracellular amyloid and the neuronal origin of Alzheimer neuritic plaques. *Neurobiol Dis* 71:53–61
141. Knopman DS et al (2021) Alzheimer disease. *Nat Rev Dis Primers* 7(1):33
142. Rosa-Ferreira C, Munro S (2011) Arl8 and SKIP act together to link lysosomes to kinesin-1. *Dev Cell* 21(6):1171–1178
143. Farias GG et al (2017) BORC/kinesin-1 ensemble drives polarized transport of lysosomes into the axon. *Proc Natl Acad Sci U S A* 114(14):E2955–E2964
144. Roney JC et al (2021) Lipid-mediated motor-adaptor sequestration impairs axonal lysosome delivery leading to autophagic stress and dystrophy in Niemann-Pick type C. *Dev Cell* 56(10):1452–1468
145. Cataldo AM, Hamilton DJ, Nixon RA (1994) Lysosomal abnormalities in degenerating neurons link neuronal compromise to senile plaque development in Alzheimer disease. *Brain Res* 640(1–2):68–80
146. Cataldo AM et al (1990) Lysosomal proteinase antigens are prominently localized within senile plaques of Alzheimer's disease: evidence for a neuronal origin. *Brain Res* 513(2):181–192
147. Hassiotis S et al (2018) Lysosomal LAMP1 immunoreactivity exists in both diffuse and neuritic amyloid plaques in the human hippocampus. *Eur J Neurosci* 47(9):1043–1053
148. Kowa H et al (2004) Mostly separate distributions of CLAC- versus Abeta40- or thioflavin S-reactivities in senile plaques reveal two distinct subpopulations of beta-amyloid deposits. *Am J Pathol* 165(1):273–281

Publisher's Note

Springer Nature remains neutral with regard to jurisdictional claims in published maps and institutional affiliations.